mathematics

MDPI

Article

# Modified Artificial Ecosystem-Based Optimization for Multilevel Thresholding Image Segmentation

**Ahmed A. Ewees [1,2], Laith Abualigah [3,4], Dalia Yousri [5], Ahmed T. Sahlol [2], Mohammed A. A. Al-qaness [6], Samah Alshathri [7,*] and Mohamed Abd Elaziz [8,9,10]**

[1] Department of e-Systems, University of Bisha, Bisha 61922, Saudi Arabia; ewees@du.edu.eg
[2] Department of Computer, Damietta University, Damietta 34511, Egypt; atsegypt@du.edu.eg
[3] Faculty of Computer Sciences and Informatics, Amman Arab University, Amman 11953, Jordan; aligah.2020@gmail.com
[4] School of Computer Sciences, Universiti Sains Malaysia, Gelugor 11800, Malaysia
[5] Electrical Engineering Department, Faculty of Engineering, Fayoum University, Faiyum 63514, Egypt; day01@fayoum.edu.eg
[6] State Key Laboratory for Information Engineering in Surveying, Mapping and Remote Sensing, Wuhan University, Wuhan 430079, China; alqaness@whu.edu.cn
[7] Department of Information Technology, College of Computer and Information Sciences, Princess Nourah Bint Abdulrahman University, Riyadh 84428, Saudi Arabia
[8] Department of Mathematics, Faculty of Science, Zagazig University, Zagazig 44519, Egypt; abd_el_aziz_m@yahoo.com
[9] Artificial Intelligence Research Center (AIRC), Ajman University, Ajman 346, United Arab Emirates
[10] School of Computer Science and Robotics, Tomsk Polytechnic University, 634050 Tomsk, Russia
* Correspondence: sealshathry@pnu.edu.sa

check for updates

**Citation:** Ewees, A.A.; Abualigah, L.; Yousri, D.; Sahlol, A.T.; Al-qaness, M.A.A.; Alshathri, S.; Elaziz, M.A. Modified Artificial Ecosystem-Based Optimization for Multilevel Thresholding Image Segmentation. *Mathematics* **2021**, *9*, 2363. https://doi.org/10.3390/math9192363

Academic Editor: Dumitru Baleanu

Received: 12 July 2021
Accepted: 15 September 2021
Published: 23 September 2021

**Abstract:** Multilevel thresholding is one of the most effective image segmentation methods, due to its efficiency and easy implementation. This study presents a new multilevel thresholding method based on a modified artificial ecosystem-based optimization (AEO). The differential evolution (DE) is applied to overcome the shortcomings of the original AEO. The main idea of the proposed method, artificial ecosystem-based optimization differential evolution (AEODE), is to employ the operators of the DE as a local search of the AEO to improve the ecosystem of solutions. We used benchmark images to test the performance of the AEODE, and we compared it to several existing approaches. The proposed AEODE achieved a high performance when evaluated by the structural similarity index (SSIM), peak signal-to-noise ratio (PSNR), and fitness values. Moreover, the AEODE outperformed the basic version of the AEO concerning SSIM and PSNR by 78% and 82%, respectively, which reserves the best features for each of AEO and DE.

**Keywords:** image segmentation; multilevel thresholding; artificial ecosystem-based optimization (AEO); differential evolution (DE); optimization algorithms

## 1. Introduction

Image segmentation is one of the primary and essential operations for pattern recognition and image analysis. Over the past years, various segmentation techniques have been introduced to improve the segmentation processes, such as fuzzy c-means, fuzzy clustering algorithms, and mean-shift analysis. The image thresholding approach is a successful and standard image segmentation method among other similar segmentation techniques. This is because of its clarity, robustness, and efficiency, which transforms a gray level image into a binary level image [1]. It is the process of partitioning an image into its component objects or regions based on color, size, shape, position, or texture [2].

There are several image segmentation techniques. However, multilevel thresholding is the most successful technique employed for segmentation purposes of different types of images out of all the current techniques [3]. The motivations behind the widespread application of multilevel thresholding are due to its simplicity and computation efficiency. It is employed to recognize and obtain a target from the image background depending on the allocation of gray levels or texture in image components (objects). So, understanding or interpretation of a given image needs to precisely segment it into vital regions [4]. Therefore, it plays a vital role in computer vision domains.

Thresholding methods are divided into local and global methods. The global methods are arranged in terms of the clustering-based information into spatial-based, entropy-based, object attribute-based, and histogram shape-based methods [5]. These methods are usually divided into two types: bi-level and multilevel [6]. In the bi-level, the image is divided into two categories [7]. In contrast, multilevel is utilized for detailed image segmentation because it provides multiple levels, such as quad-level or tri-level, and breaking pixels into multilevel depending on the image's pixels. Therefore, image segmentation by multilevel thresholding has drawn more consideration because of its various applications in different fields [8]. However, determining the optimal threshold value is still the most challenging problem encountered in thresholding techniques, and it needs further investigation.

For a precise description of the thresholds, different variance measures as the entropy are employed. Two conventional techniques are the intra-class variance [9] and Kapur's entropy [10]. These techniques are beneficial in obtaining a single threshold. However, conventional techniques suffer from some limitations, such as computational time. In addition to that, the complexity rises considerably when dividing the image into more than two classes is necessary. The applications of meta-heuristic optimization methods were proposed in many studies to address this problem, which presented good results [11].

Optimization algorithms are promising mechanisms to perform complicated optimization tasks with a high level of accuracy [12]. In the published literature, several methods were proposed for multilevel thresholding, such as the stochastic fractal search (SFS) algorithm, spherical search optimization (SSO) algorithm, artificial bee colony (ABC) algorithm, sine–cosine algorithm (SCA), differential evolution (DE) algorithm, multi-verse optimization (MVO) algorithm, particle swarm optimization (PSO) algorithm, whale optimization algorithm (WOA), genetic algorithm (GA), social spider optimization (SSO), honey bee mating optimization (HBMO), flower pollination algorithm (FPA) algorithm, crow search algorithm (CSA), and world cup optimization (WCO) algorithm [13]. However, as every image is considered an optimization problem, not all optimization algorithms give precise results by applying the Otsu and Kapur as objective functions. In particular, an algorithm can obtain the optimal configuration of thresholds for a particular image but not for all given images.

Zhao et al. in [14] proposed a new optimization algorithm inspired by nature, called artificial ecosystem-based optimization (AEO). This algorithm is a warm-based search method driven by the flow of power in an environment on the ground, and it simulates three different styles of living organisms: production, consumption, and decomposition. The authors experimented using different test functions and optimization tasks. The results showed that the AEO has an advantage over other equivalents. AEO is superior to other comparative algorithms in both computational cost and convergence speed, particularly for engineering applications. In general, the AEO is prevalent, which motivates us to employ it for solving multilevel thresholding problems.

This paper develops an efficient image segmentation method depending on a modified version of the AEO, using the differential evolution (DE) strategy. The proposed method, called AEODE, intends to evade the shortcomings of the conventional AEO by applying the operators of DE as an exploitation strategy (local search) to enhance the ecosystem of solutions. The power of these combined algorithms is employed for enhancing the performance of the multilevel thresholds image segmentation. DE is a search method that optimizes the given problem by iteratively working to enhance a solution concerning the fitness function [15]. This method was used before in many engineering problems and applications, such as engineering problems, numerical function optimization, feature selection, big data optimization problems, text clustering, reactive power dispatch problem, solar photovoltaic and wind energy, multilevel image thresholding, optimal power flow, and continuous optimization problems.

Generally, the proposed AEODE method works on calculating the histogram of the provided image. Then, it creates random candidate solutions subject to the minimum and maximum histogram values. Each candidate solution includes a collection of position values that design the threshold values. The fuzzy entropy is employed as a fitness function to assess the quality of the candidate solutions, and the best-obtained solution has the most significant fitness value. After that, the current candidate solutions are updated according to a condition with a random value to operate the AEO or DE. After completing the updating procedure for the given solutions, the terminal criteria are checked to verify whether they are satisfied or not, so the preceding steps are executed again. We implement extensive experiments, using benchmark images to evaluate the AEODE method; then, we compare it to many existing optimization methods.

Our main contribution can be summarized as follows:

- Propose an alternative multilevel thresholding image segmentation method based on hybrid AEO and DE algorithms.
- Blend the strength of the AEO and the DE to develop the proposed AEODE method for optimizing the thresholding value.
- Evaluate the efficiency of the AEODE, using a set of benchmark images.
- Compare the proposed image segmentation method with the state-of-the-art methods published in that domain.

The remainder of this paper is presented as follows. Section 2 presents the related works that studied the image segmentation problems, using optimization techniques. Section 3 presents the preliminaries of the methods. The description of the AEODE method is presented in Section 4. The experiment and comparisons are described in Section 5. Section 6 concludes the paper.

## 2. Literature Review

One of the most vital techniques utilized in the computer vision domain is multilevel thresholding. Conventional segmentation techniques suffer from difficulties in settling the proper threshold values; hence, meta-heuristic (MH) algorithms are successfully applied to address these difficulties. Generally, meta-heuristic algorithms are introduced by mimicking natural behaviors of groups in the environment, such as wild animals, flying animals, science, theories, and others. In [16], a new multilevel thresholding approach was presented based on a new version of the spherical search optimization (SSO) algorithms, called SSOSCA. The proposed method used operators from the components of the conventional SCA to improve the exploitation searchability of the conventional SSO algorithm. Fuzzy entropy was employed as the leading fitness function to assess the nature of candidate solutions of the SSOSCA. In the experiments, several images were taken from Berkeley benchmark datasets to analyze and test the performance of the SSOSCA. The results showed that the SSOSCA achieved competitive performance, compared to several existing algorithms based on various image segmentation metrics.

Horng in [17] presented a multilevel maximum entropy thresholding method, using the ABC algorithm, called (MEABCT). Four approaches were compared to the MEABCT algorithm: the PSO algorithm, cooperative–comprehensive PSO, HBMO, and Fast Otsu's approach. The evaluation results showed that the MEABCT could explore multiple threshold values near the optimal value observed by the optimization method. The segmentation results of the MEABCT algorithm are better than the other methods; nevertheless, the computation time by utilizing the proposed MEABCT is less than that of the other comparative algorithms.

Yousri et al. [18] proposed a new method to improve the search abilities of the FPA. Accordingly, fractional-order (FO) calculus characteristics were utilized to improve the exploitation searchability of the conventional FPA and adaptively enhance the harmonization parameter between the FPA exploitation and exploration search. It was tested on different test functions with various dimensions. In addition, it was compared with similar established techniques in the literature, using different statistical evaluation measures and non-parametric analyses. Moreover, it was implemented for a real-word image segmentation purposes, and the obtained results were compared to several existing methods.

Forouzanfar et al. in [19] proposed a study to examine the potential of the GA and PSO algorithms to determine the optimum value of the degree of attraction of the segmentation processes. The GA showed better performance in determining a close-optimal solution; however, it had an issue in obtaining an exact solution, while the PSO algorithm enhanced the exploration for finding the optimal solution. Consequently, vital changes are expected by utilizing a hybrid method by combining the PSO with GA algorithms. In this way, the hybrid GA-PSO algorithm is used to find the optimum degree of attraction in the image segmentation process. The quantitative and qualitative analyses are conducted on image benchmark datasets and brain MR images with various noise shapes. The results showed unique enhancements in segmentation results matched to other fuzzy c-means methods.

In [20], the authors presented a clustering approach, using PSO for image segmentation, called divergent–convergent PSO (DCPSO). The DCPSO automatically manages the number of groups and concurrently gathers the dataset with the smallest user interference. The DCPSO begins by clustering the dataset into many clusters to minimize the impacts of initial shapes. The optimal number of clusters is selected by using the binary PSO. Then, the K-means clustering algorithm perfects the centers of the determined clusters. The proposed algorithm was tested on both natural and synthetic image datasets. The results revealed that the DCPSO algorithm obtained the optimal number of clusters on the experimented image datasets, compared to other similar methods, such as GA and the conventional PSO algorithm.

In [21], a new image segmentation method is presented, using many-objective optimization: knee evolutionary algorithm (KnEA) is one of the best multi-objective methods utilized to determine solutions, using seven functions to improve the effectiveness of the segmentation process. The KnEA was assessed, utilizing several images tested at six various threshold levels, and the results were compared to several existing many-objective optimization techniques. Comparison of the results showed that the KnEA performs better in estimating the optimal solutions than other methods in terms of the computational time, and the segmented quality, such as SSIM, PSNR, coverage, hypervolume, and spacing indicators.

Smith in [22] proposed a segmentation method, using the RFC algorithm. The proposed method quantitatively assesses various possible image segmentation alternatives to distinguish the segmentation scale(s). The selection process of the image segmentation rule was utilized to distinguish between three basic image object rules after combination. Then, the RFC algorithm was applied to determine the land cover classes to 11 gray-scale images of SPOT satellite imagery. The results showed that the RFC algorithm achieved better performance with an average accuracy of 85.2%. In another study, Shahrezaee [23] proposed an image segmentation approach based on the WCO algorithm. The proposed approach used the WCO to analyze the original pixels of images into various groups. The performance of the WCO was evaluated and compared to several existing approaches, such as Otsu, GA, and PSO, and it achieved good performance.

In [24], the authors proposed a multi-objective optimization method, using the MVO algorithm for gray-scale image segmentation by multi-thresholding values. An approximate Pareto-optimal set was involved in increasing the Otsu and Kapur objective functions in their method. These functions are usually employed in solving image segmentation through bi-level and multi-level thresholding. Nevertheless, each function has specific conditions and properties. Several optimization algorithms were introduced to optimize these functions in terms of efficiency independently. In contrast, just a few multi-objective methods have investigated the advantages of utilizing a combination of Otsu and Kapur. However, the computational damage of Otsu and Kapur is extensive, and their efficiency needs to be enhanced. Eleven gray-scale images were utilized to test the multi-objective

MVO. Moreover, it was compared with three different multi-objective methods, and it obtained significant performance.

In conclusion, we notice that optimization-based multilevel thresholding image segmentation is considered an emerging research field with new and exciting theories and strategies. It is also recognized as a critical problem to employ various techniques with various objective functions over varying models of images.

## 3. Background

### *3.1. Problem Definition*

In this section, we briefly define the problem of multilevel thresholding. If we have $I$ gray-scale image, it will have $K+1$ classes. For dividing the $I$ image into classes, we need the values of $k$ thresholds $\{t_k, k = 1, 2, K\}$, and this can be formulated as follows [25]:

$$\begin{aligned} C_0 &= \{I_{ij} \mid 0 \leq I_{ij} \leq t_1 - 1\}, \\ C_1 &= \{I_{ij} \mid t_1 \leq I_{ij} \leq t_2 - 1\}, \\ &\dots \\ C_K &= \{I_{ij} \mid t_K \leq I_{ij} \leq L - 1\} \end{aligned} \tag{1}$$

in which $L$ is the maximum gray levels, and $C_K$ is a $k$th class of the $I$. The $t_k$ is the $k$-th threshold, where $I_{ij}$ is a gray level at $(i, j)$-th pixel. Moreover, a multilevel thresholding problem is defined as a maximization problem that is employed to find the optimal threshold, as given by Equation (2):

$$t_1^*, t_2^*, \dots, t_K^* = \arg \max_{t_1,\dots,t_K} Fit(t_1, \dots, t_K) \tag{2}$$

where $Fit$ represents the objective function. In this paper, we use fuzzy entropy [9] as the objective function. Fuzzy entropy was used in various segmentation approaches [26,27], and it can be formulated as follows:

$$Fit(t_1, \dots, t_K) = \sum_{k=1}^{K} H_i \tag{3}$$

$$H_k = -\sum_{i=0}^{L-1} \frac{p_i \times \mu_k(i)}{P_k} \times ln(\frac{p_i \times \mu_k(i)}{P_k}), \tag{4}$$

$$P_k = \sum_{i=0}^{L-1} p_i \times \mu_k(i) \tag{5}$$

$$\mu_1(l) = \begin{cases} 1 & l \leq a_1 \\ \frac{l-c_1}{a_1-c_1} & a_1 \leq l \leq c_1 \\ 0 & l > c_1 \end{cases} \tag{6}$$

$$\mu_K(l) = \begin{cases} 1 & l \leq a_{K-1} \\ \frac{l-a_K}{c_K-a_K} & a_{K-1} < l \leq c_{K-1} \\ 0 & l > c_{K-1} \end{cases}$$

where $p_i$ is the probability distribution, which is computed as $p_i = h(i)/N_p$ $(0 < i < L-1)$. $h(i)$ and $N_p$ represent pixel numbers for the corresponding gray level $L$ and total pixel numbers of the $I$. Furthermore, $a_1, c_1, \dots, a_{k-1}, c_{k-1}$ represent the fuzzy parameters, and $0 \leq a_1 \leq c_1 \leq \dots \leq a_{K-1} \leq c_{K-1}$. Then $t_1 = \frac{a_1+c_1}{2}, t_2 = \frac{a_2+c_2}{2}, \dots, t_{K-1} = \frac{a_{K-1}+c_{K-1}}{2}$. The relevant fitness value is the highest one.

### 3.2. Differential Evolution (DE)

Storn and Price [15] presented the DE as a first attempt in 1997 for solving several optimization problems. DE is distinguished by its flexibility, short execution time, rabid acceleration trend, and its fast and precise local operator for selection. The optimization process in DE starts with a random set of solutions for discovering most of the points in the search space (initialization phase). After that, the solutions can be modified based on a set of operators, which are *mutation* and *crossover*, and then the agent solution is upgraded when the newly generated solution achieves a better objective value. The mathematical model of the mutation operator $Z_i^t$ can be implemented for the current individual $XD_i$ as below:

$$Z_i^t = XD_{rand_1}^t + F \times (XD_{rand_2}^t - XD_{rand_3}^t), \tag{7}$$

where $rand_1, rand_2$, and $rand_3$ are random indexes that are varied from the current index $i$. $F$ is the mutation scaling factor, and it has a value greater than 0. The symbol of $t$ refers to the iteration number.

For the crossover operator, Equation (8), below, illustrates that during the crossover process, a new solution vector $V_i$ is created based on the mutated individual $Z_i$ and the solutions vector $XD_i$. The crossover process is accounted for as a mixture between vectors $Z_i$ and $XD_i$, where the diversity of the agents is enhanced.

$$V_i^t = \begin{cases} zi^t & if\ rand \leq C_r \\ XD_i^t & otherwise \end{cases} \tag{8}$$

where $rand$ is a random value in the [0, 1] interval, and $C_r$ is the crossover probability.

The final phase in the DE algorithm is upgrading the agents' solutions based on the attained objective values, where the generated individual $V_i^t$ is exchanged with the current individual if it has a better objective as follows:

$$XD_i^{t+1} = \begin{cases} V_i^t & if\ f(v_i^t) < f(XD_i^t) \\ XD_i^t & otherwise \end{cases} \tag{9}$$

These steps are repeated until the stopping criteria are met.

### 3.3. Artificial Ecosystem-Based Optimization

AEO is a new optimization method inspired by the chain energy transfer among living organisms [14]. This process happens through three sequential processes: production, consumption, and decomposition. Zhao et al. [14] represented these processes mathematically to achieve optimal solutions for several optimization problems; thus, the AEO optimizer was proposed. The production process is responsible for improving the balance among the diversification and intensification perspectives in AEO, whereas for discovering the total search space, the consumption operator is implemented (diversification perspective). The intensification perspective can be excluded in the decomposition process. In AEO, the producer (plants) and decomposer (fungi and bacteria) are only one agent, while the rest of the agents can be considered consumers that can be classified based on their diet. These animal types are (1) herbivores (eat plants), (2) omnivores (eat plants and other animals), and (3) carnivores (eat only other animals). The agents in this hierarchy update their positions, according to the following equations.

1. Production process: Zhao et al. [14] considered the producer as the worst agent in the populations. In AEO, the producer updates its location depending on randomly selected individual in the search space, as well as the decomposed (best agent) as presented below:

$$X_1(t+1) = (1-d)X_n(t) + d \cdot X_{rand}(t) \tag{10}$$

$$d = (1 - \frac{t}{T_{max}})rand_1 \tag{11}$$

$$X_{rand}(t) = rand_2() \cdot (I_{max} - I_{min}) + lb, \tag{12}$$

where $I_{max}$ and $I_{min}$ are the upper and lower boundaries of the search space, respectively. $t$ and $T_{max}$ refer to the iteration number and the maximum number of iterations, respectively. $rand_1$ and $rand_2$ represent random values withdrawn from the [0, 1] interval, and $d$ represents a weight coefficient.

2. Consumption process: in this stage, the consumer feeds on another consumer with a lower level of energy or on a producer. For the consumer classes, carnivores, herbivores, and omnivores, each one has its specific tactic for updating the location as illustrated below:

   (a) Herbivore consumers update their locations depending on the producers only (feed on the producers).

   $$X_i(t+1) = X_i(t) + G \cdot (X_i(t) - X_1(t)) \tag{13}$$

   where producer $X_1$ represents the producer location, and $G$ represents a consumption factor, which is computed using levy flight as follows:

   $$G = \frac{1}{2}\frac{u}{v}, u \in Norm(0,1), v \in Norm(0,1) \tag{14}$$

   where $Norm(0,1)$ represents the normal distribution with zero mean and unit variance.

   (b) Carnivore consumers update their locations using a random consumer with high-level energy with an index $(ind)$, as carnivores feed on other animals only as mentioned earlier. The carnivore location can be formulated as follows:

   $$X_i(t+1) = X_i(t) + G \cdot (X_i(t) - X_{ind}(t)) \tag{15}$$

   $$ind = randi([2\,i-1]), i = 3, \ldots, N, \tag{16}$$

   (c) Omnivore consumers update their locations depending on the producer and randomly selected consumer with index $(ind)$ with a higher level of energy as modeled below:

   $$X_i(t+1) = X_i(t) + G \cdot X_{ra} + X_{ra2}, \tag{17}$$

   $$X_{ra} = (rand_3 \cdot (X_i(t) - X_1(t))), \tag{18}$$

   $$X_{ra2}(1 - rand_3) \cdot (X_i(t) - X_{ind}(t)), \tag{19}$$

   $$ind = randi([2\,i-1]), i = 3, \ldots, N, \tag{20}$$

3. Decomposition process: this is the final process of the ecosystem as each individual in the agent dies, and the decomposer starts breaking down its remains. Zhao et al. [14] considered it to be the intensification phase of AEO and modeled it as follows:

$$X_i(t+1) = X_i(t) + D \cdot (e \cdot X_n(t) - q \cdot X_i(t)), \tag{21}$$

$$D = 3u, \quad u \in N(0,1) \tag{22}$$

$$e = rand_4 \cdot randi([1 \quad 2]) - 1, \tag{23}$$

$$q = 2 \cdot rand_5 - 1, \tag{24}$$

where the decomposition factor is represented by $D$, and weight parameters are represented by $e$ and $q$.

## 4. The Proposed AEODE

The structure of the proposed method based on modified the AEO using DE is given in Figure 1. The developed AEODE uses the operators of DE to enhance the exploitation of

AEO. It has the largest effect on AEO performance and provides it with suitable operators to avoid the attractiveness to a local point.

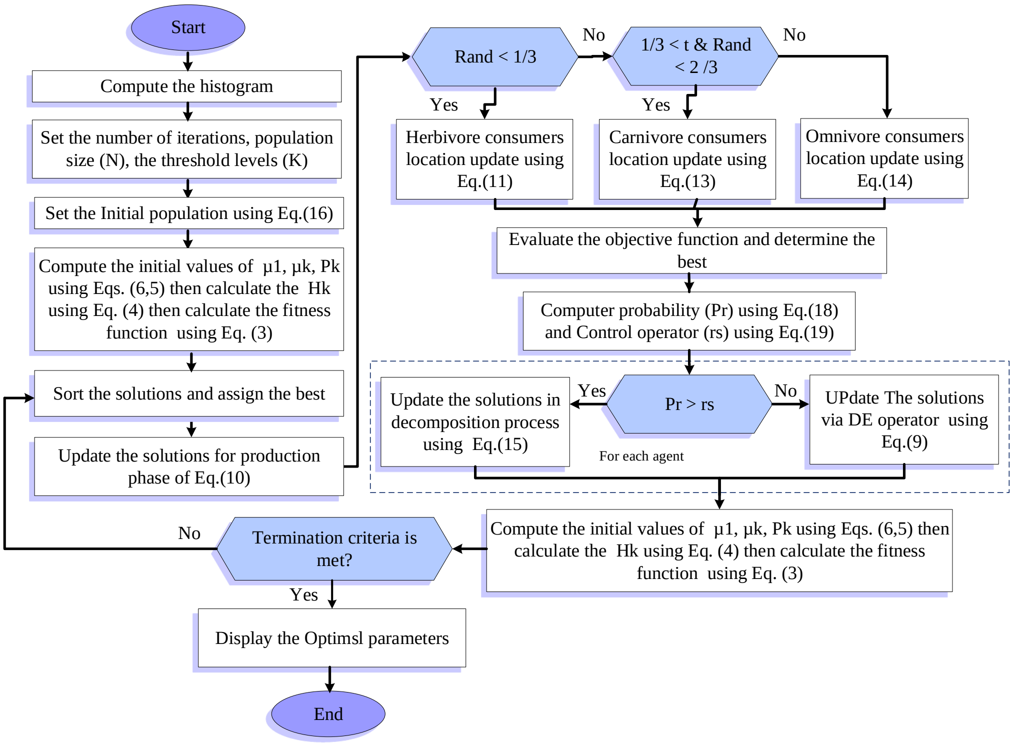
Start
Compute the histogram
Set the number of iterations, population size (N), the threshold levels (K)
Set the Initial population using Eq.(16)
Compute the initial values of µ1, µk, Pk using Eqs. (6,5) then calculate the Hk using Eq. (4) then calculate the fitness function using Eq. (3)
Sort the solutions and assign the best
Update the solutions for production phase of Eq.(10)
Rand < 1/3
No
1/3 < t & Rand < 2 /3
No
Yes
Yes
Herbivore consumers location update using Eq.(11)
Carnivore consumers location update using Eq.(13)
Omnivore consumers location update using Eq.(14)
Evaluate the objective function and determine the best
Computer probability (Pr) using Eq.(18) and Control operator (rs) using Eq.(19)
Update the solutions in decomposition process using Eq.(15)
Yes
Pr > rs
No
UPdate The solutions via DE operator using Eq.(9)
For each agent
Compute the initial values of µ1, µk, Pk using Eqs. (6,5) then calculate the Hk using Eq. (4) then calculate the fitness function using Eq. (3)
No
Termination criteria is met?
Yes
Display the Optimsl parameters
End

**Figure 1.** The flowchart of the AEODE.

In general, the developed AEODE begins by using Equation (25) to generate the initial population $X$ as shown in the following equation:

$$X_{i,j} = I_{min,j} + r_1 \times (I_{max,j} - I_{min,j}), \quad i = 1, 2, \ldots, N \tag{25}$$

In Equation (25), the value of $I_{max,j}$ and $I_{min,j}$ represent the maximum and minimum gray value of $I$ at dimension $j$, respectively, whereas $Dim = 2K$ is the dimension of each solution (here $K$ refers to the threshold levels used to segment $I$). Therefore, the best solution $X_b$ is allocated, followed by updating the value of other solutions.

The process of updating solutions is implemented, using the operators of the traditional AEO algorithm during the exploration. However, in the case of the solutions that go through the exploitation phase, they will be updated using either the operators of AEO or DE, using the following equation:

$$X_i = \begin{cases} operators\, of\; AEO & Pr_i > r_s \\ operators\, of\; DE & otherwise \end{cases} \tag{26}$$

In Equation (26), $Pr_i$ is the probability of each $X_i$ and it depends on the fitness value ($Fit_i$, which is defined in Equation (3). The formulation of $Pr_i$ is given as follows:

$$Pr_i = \frac{Fit_i}{\sum_{i=1}^{N} Fit_i} \tag{27}$$

where

$$r_s = min(Pr_i) + rand \times (max(Pr_i) - min(Pr_i)), \; rand \in [0, 1] \tag{28}$$

The main objective of using $r_s$ is a variable that controls the process of using the operators of DE and AEO. To avoid the problem of making it a constant value since it is expected that the value of $Pr_i$ is increased with excess iterations, the operators of AEO are used only, especially at the end of iterations. Therefore, we update dynamically the value of $r_s$ according to the probability of each solution. This gives the developed AEODE high flexibility in switching between AEO and DE.

The next process in AEODE is to check the terminal criteria and return by the best solution when they are reached (i.e., here, the maximum number of iterations), followed by extracting the threshold values from $X_b$ as $t_k = \frac{X_b^k + X_b^{k+1}}{2}$, $k = 1:2:K-1$.

*Complexity of AEODE*

The complexity of the AEODE, in general, depends on the complexity of traditional AEO, quick sort (QS), and DE. Since the complexity of DE is given as

$$O(DE) = O((N \times D + N \times D + N) \times t_{max}) \tag{29}$$

Therefore, the complexity of AEODE is given as follows:

$$O(AEODE) = O(t_{max} \times (Term1 + Term2)) \tag{30}$$

$$Term1 = (QS + N \times D + N \times D + N)$$

$$Term2 = ((N_K \times D + N_K \times D + N_K) + (N - N_K) \times D)$$

In the best case of QS, the complexity of AEODE is given as follows:

$$O(AEODE) = O(t_{max} \times (NlogN + N \times D + N_K \times D + N_K)) \tag{31}$$

In the worst case of QS, the complexity of AEODE is given as follows:

$$O(AEODE) = O\Big(t_{max} \times (N^2 + N \times D + N_K \times D + N_K)\Big) \tag{32}$$

where $N_K$ is the number of solutions updated, using DE.

## 5. Evaluation Experiment

We compare the proposed AEODE method with relevant approaches to segment 10 standard test images, as shown in Figure 2. In addition, the histogram of each image is given in Figure 2 which indicates the characteristic of each image. Swarm parameters are adjusted to their original implementations [28]. The number of population is set to 20, while the dimension equals the threshold level. Moreover, the iteration number is set to 100, and all parameters are selected, depending on the recommendation by the authors of [29].

Several threshold values were adopted to test the proposed approach (i.e., 6, 8, 15, 17, 19, and 25). The performance of the AEODE was obtained by applying it on several images that are variant in shape, morphology, and contents. The experiments were implemented, using Matlab 2014b on a computer “Core i5 and 8 GB of RAM running on MS Windows 10”.

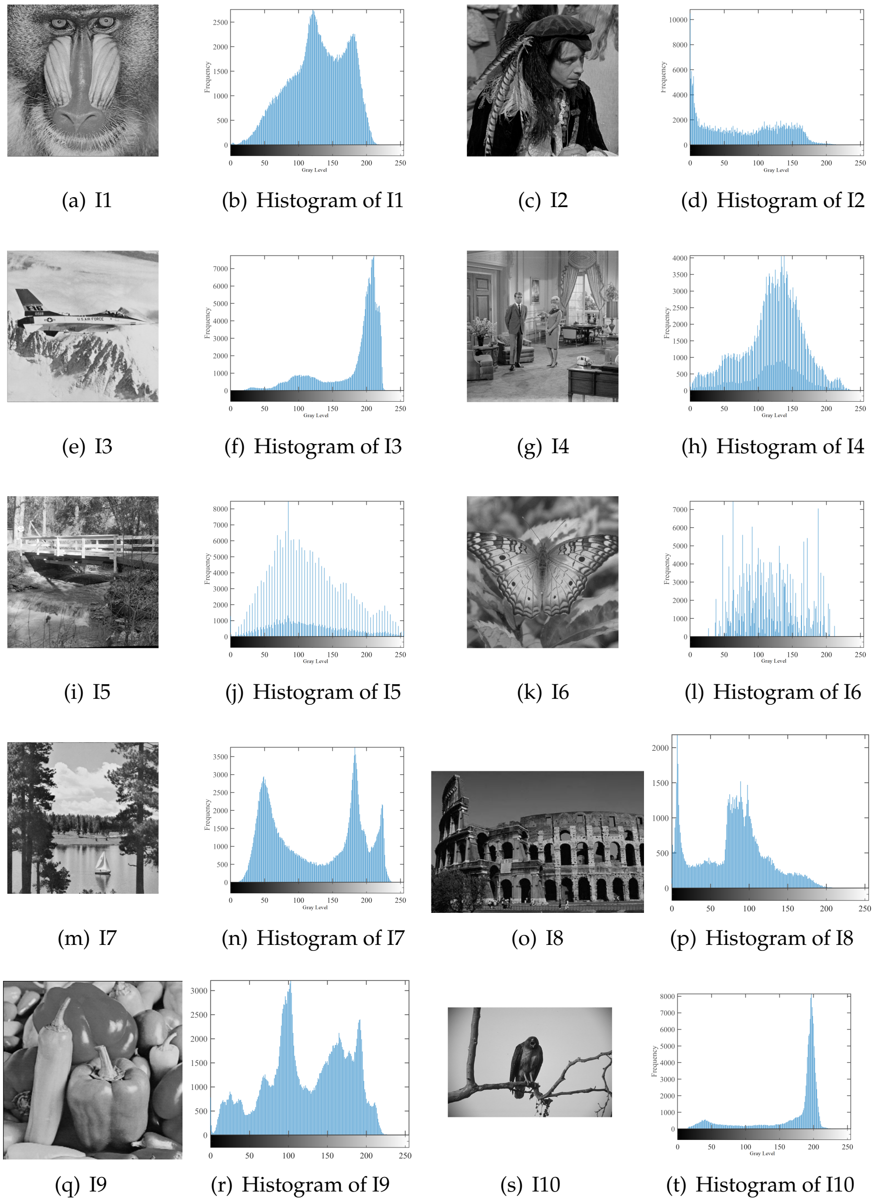

(a) I1 (b) Histogram of I1 (c) I2 (d) Histogram of I2

(e) I3 (f) Histogram of I3 (g) I4 (h) Histogram of I4

(i) I5 (j) Histogram of I5 (k) I6 (l) Histogram of I6

(m) I7 (n) Histogram of I7 (o) I8 (p) Histogram of I8

(q) I9 (r) Histogram of I9 (s) I10 (t) Histogram of I10

**Figure 2.** Tested images with their histograms.

### 5.1. Performance Measures

We evaluate the performance of the AEODE using three performance measures, called the fitness function value, the structural similarity index (SSIM), and the peak signal-to-noise ratio (PSNR). SSIM and PSNR are computed by the following equations:

$$SSIM(I, I_S) = \frac{(2\mu_I \mu_{I_S} + c_1)(2\sigma_{I,I_S} + c_2)}{(\mu_I^2 + \mu_{I_S}^2 + c_1)(\sigma_I^2 + \sigma_{I_S}^2 + c_2)} \tag{33}$$

where $\mu_{I_S}$ $(\sigma_{I_S})$ and $\mu_I(\sigma_I)$ represent images' mean intensity of $I_S$ and $I$, respectively. $\sigma_{I,I_S}$ defines the covariance of $I$ and $I_S$. $c_1$ and $c_2$ are equal to 6.5025 and 58.52252, respectively [30].

$$PSNR = 20log_{10}(\frac{255}{RMSE}), \tag{34}$$

$$RMSE = \sqrt{\frac{\sum_{i=1}^{N_r} \sum_{j=1}^{N_c} (I_{i,j} - I_S i, j)^2}{N_r \times N_c}}$$

where $RMSE$ refers to the root mean-squared error.

### *5.2. Results and Discussion*

The proposed AEODE method is tested besides other optimization algorithms, such as the basic artificial ecosystem-based optimization (AEO), marine predators algorithm (MPA), gray wolf optimization (GWO), spherical search optimization (SSO), cuckoo search (CS), and grasshopper optimization algorithm (GOA). The results can be divided mainly into three main categories, as follows.

#### 5.2.1. Performance Measure by Structural Similarity Index (SSIM)

Figure 3 and Table 1 show the results of our AEODE method, compared to the most recent optimization algorithms based on SSIM measure.

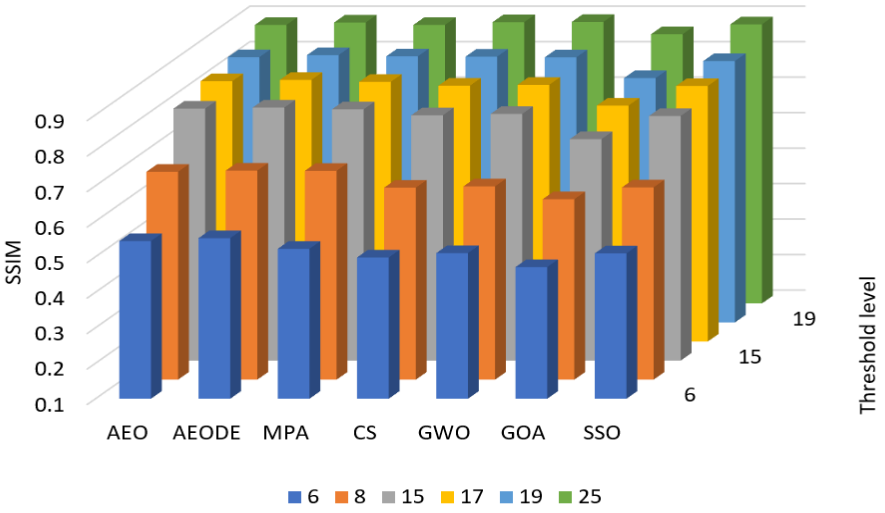

**Figure 3.** SSIM at different threshold levels.

Figure 3 shows that the AEODE performs better in both of the low thresholding levels (i.e., 5 and 6) and also in the higher thresholding levels (i.e., 19 and 25), while GOA shows the lowest performance among other optimization algorithms.

Table 1 shows the SSIM values performed by each optimization algorithm for each image with different threshold levels. From Table 1, we see that the AEODE method allocates the first rank (the highest SSIM values at 25 cases), followed by MPA and CS algorithms (eight highest SSIM values for each), which provide better results than others. Additionally, AEODE achieved good SSIM values in all threshold levels.

**Table 1.** SSIM results for all algorithms (bold means the best value).

| Threshold | Image | AEO | AEODE | MPA | CS | GWO | SSA | GOA | SSO |
|---|---|---|---|---|---|---|---|---|---|
| 6 | I1 | 0.53396 | **0.5618** | 0.50579 | 0.52352 | 0.51025 | 0.39938 | 0.48972 | 0.53913 |
| | I2 | 0.44281 | 0.43436 | 0.41918 | 0.40398 | 0.40233 | **0.52873** | 0.38488 | 0.40887 |
| | I3 | 0.6135 | 0.62192 | 0.59835 | 0.61624 | 0.60716 | **0.64755** | 0.61252 | 0.63662 |
| | I4 | 0.52059 | 0.52952 | 0.48349 | 0.5448 | **0.55125** | 0.52551 | 0.53858 | 0.53506 |
| | I5 | 0.39568 | **0.4004** | 0.37672 | 0.29943 | 0.31531 | 0.39835 | 0.24689 | 0.35574 |
| | I6 | 0.4401 | **0.45909** | 0.41752 | 0.3415 | 0.36174 | 0.39093 | 0.30873 | 0.38448 |
| | I7 | 0.45267 | 0.46214 | 0.4291 | 0.41906 | 0.4188 | **0.54524** | 0.39571 | 0.42966 |
| | I8 | 0.56102 | 0.56591 | 0.54474 | 0.59211 | 0.57265 | **0.64572** | 0.54101 | 0.57902 |
| | I9 | 0.7241 | **0.73382** | 0.71886 | 0.57796 | 0.70238 | 0.71535 | 0.56442 | 0.54372 |
| | I10 | 0.75823 | 0.75492 | 0.73026 | 0.66034 | 0.66138 | **0.77956** | 0.62704 | 0.68312 |

**Table 1.** *Cont.*

| Threshold | Image | AEO | AEODE | MPA | CS | GWO | SSA | GOA | SSO |
|---|---|---|---|---|---|---|---|---|---|
| 8 | I1 | 0.72614 | 0.72068 | 0.71035 | 0.71459 | 0.70441 | 0.54141 | 0.68052 | 0.70587 |
| | I2 | 0.55282 | 0.56874 | **0.58633** | 0.45404 | 0.45667 | 0.52761 | 0.40373 | 0.46437 |
| | I3 | 0.72347 | 0.72196 | 0.70095 | **0.76111** | 0.75279 | 0.65808 | 0.75203 | 0.77642 |
| | I4 | 0.645 | 0.65213 | **0.65855** | 0.60049 | 0.58887 | 0.55473 | 0.57312 | 0.60482 |
| | I5 | 0.63042 | **0.63415** | 0.63535 | 0.55223 | 0.56527 | 0.52105 | 0.53659 | 0.53372 |
| | I6 | 0.6327 | **0.63537** | 0.6475 | 0.51139 | 0.5342 | 0.41109 | 0.44601 | 0.53234 |
| | I7 | 0.61356 | 0.61623 | **0.6379** | 0.58497 | 0.56852 | 0.58721 | 0.53671 | 0.58961 |
| | I8 | 0.72496 | **0.73439** | 0.71537 | 0.64796 | 0.70713 | 0.64018 | 0.63638 | 0.63361 |
| | I9 | 0.77189 | 0.76749 | 0.77213 | **0.80557** | 0.80464 | 0.74337 | 0.78055 | 0.80571 |
| | I10 | 0.8359 | **0.83796** | 0.81993 | 0.77708 | 0.76321 | 0.79199 | 0.73836 | 0.76977 |
| 15 | I1 | 0.84257 | **0.84348** | 0.83516 | 0.8378 | 0.81281 | 0.6043 | 0.79505 | 0.83572 |
| | I2 | 0.70787 | **0.72741** | 0.72224 | 0.67424 | 0.70364 | 0.58825 | 0.58646 | 0.66409 |
| | I3 | 0.82551 | 0.82882 | 0.78965 | **0.85413** | 0.84984 | 0.7061 | 0.82652 | 0.8465 |
| | I4 | **0.76668** | 0.76218 | 0.76217 | 0.73951 | 0.74846 | 0.58438 | 0.68076 | 0.76032 |
| | I5 | 0.80116 | **0.80893** | 0.798 | 0.76274 | 0.78447 | 0.55193 | 0.67289 | 0.76257 |
| | I6 | **0.76882** | 0.76403 | 0.75681 | 0.74085 | 0.72203 | 0.43352 | 0.61737 | 0.75585 |
| | I7 | 0.76895 | 0.77076 | 0.78581 | 0.76759 | **0.79293** | 0.61501 | 0.64608 | 0.76416 |
| | I8 | 0.84272 | 0.83542 | **0.84811** | 0.8248 | 0.83539 | 0.68349 | 0.76642 | 0.82585 |
| | I9 | 0.86649 | **0.87485** | 0.8676 | 0.84894 | 0.8542 | 0.8011 | 0.82481 | 0.83208 |
| | I10 | 0.90939 | 0.91455 | **0.9152** | 0.86198 | 0.84617 | 0.81927 | 0.82345 | 0.84518 |
| 17 | I1 | 0.86894 | 0.86292 | 0.85717 | **0.87164** | 0.8434 | 0.59045 | 0.83058 | 0.86417 |
| | I2 | 0.7478 | **0.76251** | 0.75533 | 0.73452 | 0.75615 | 0.54872 | 0.61554 | 0.72061 |
| | I3 | 0.84686 | 0.83269 | 0.82665 | 0.86869 | 0.86657 | 0.72056 | 0.85029 | **0.87188** |
| | I4 | 0.78076 | **0.80353** | 0.79274 | 0.77364 | 0.77225 | 0.56542 | 0.72636 | 0.77225 |
| | I5 | 0.83757 | **0.84195** | 0.83266 | 0.81014 | 0.82748 | 0.60601 | 0.74483 | 0.80114 |
| | I6 | 0.79235 | **0.79536** | 0.78603 | 0.77734 | 0.77474 | 0.47968 | 0.67667 | 0.80482 |
| | I7 | 0.80524 | 0.81419 | 0.79872 | 0.78759 | **0.81934** | 0.62238 | 0.72879 | 0.7812 |
| | I8 | 0.86742 | **0.87129** | 0.87037 | 0.84137 | 0.8635 | 0.68178 | 0.79223 | 0.85152 |
| | I9 | 0.86965 | **0.87394** | 0.87281 | 0.85917 | 0.85488 | 0.8118 | 0.83079 | 0.85502 |
| | I10 | 0.91904 | 0.91465 | **0.92399** | 0.88497 | 0.85498 | 0.83222 | 0.85329 | 0.87835 |
| 19 | I1 | **0.87635** | 0.88501 | 0.87613 | 0.883 | 0.86528 | 0.59886 | 0.84743 | 0.88062 |
| | I2 | 0.76872 | 0.77978 | **0.78149** | 0.7644 | 0.78806 | 0.59244 | 0.66842 | 0.74173 |
| | I3 | 0.85051 | 0.84382 | 0.83837 | 0.87621 | 0.87408 | 0.69963 | 0.85775 | **0.87997** |
| | I4 | 0.81724 | **0.83029** | 0.82357 | 0.79278 | 0.80193 | 0.55642 | 0.73432 | 0.78558 |
| | I5 | 0.86194 | **0.86551** | 0.84376 | 0.85091 | 0.85249 | 0.57686 | 0.78763 | 0.82448 |
| | I6 | 0.81372 | 0.81319 | 0.81469 | **0.8361** | 0.80929 | 0.49202 | 0.71495 | 0.81491 |
| | I7 | 0.82006 | 0.82438 | 0.83027 | 0.83388 | **0.84005** | 0.64693 | 0.76148 | 0.82062 |
| | I8 | 0.87385 | **0.88711** | 0.87839 | 0.87664 | 0.88092 | 0.72755 | 0.80646 | 0.86929 |
| | I9 | 0.88497 | **0.88746** | 0.88334 | 0.87026 | 0.87113 | 0.81153 | 0.83718 | 0.86986 |
| | I10 | 0.90722 | 0.91623 | **0.92831** | 0.90501 | 0.88699 | 0.82973 | 0.87028 | 0.87877 |
| 25 | I1 | 0.91122 | **0.91809** | 0.91088 | 0.91508 | 0.90582 | 0.64155 | 0.8951 | 0.91449 |
| | I2 | 0.82578 | 0.83129 | 0.82393 | 0.83724 | **0.8647** | 0.63701 | 0.79231 | 0.8200 |
| | I3 | 0.86761 | 0.88327 | 0.88309 | **0.90407** | 0.90137 | 0.7196 | 0.88303 | 0.89804 |
| | I4 | 0.86909 | **0.87565** | 0.85928 | 0.86056 | 0.85436 | 0.60861 | 0.82264 | 0.85181 |
| | I5 | 0.90929 | 0.91231 | 0.90371 | **0.91259** | 0.91112 | 0.60574 | 0.86639 | 0.89367 |
| | I6 | 0.86516 | 0.87165 | 0.86501 | 0.87474 | 0.88643 | 0.57681 | 0.82227 | **0.8918** |
| | I7 | 0.86834 | 0.87462 | 0.86578 | **0.87983** | 0.87767 | 0.66865 | 0.84386 | 0.87017 |
| | I8 | 0.91503 | **0.91964** | 0.91417 | 0.9118 | 0.91455 | 0.75603 | 0.88377 | 0.90359 |
| | I9 | 0.90205 | **0.90818** | 0.90161 | 0.90348 | 0.8934 | 0.81819 | 0.87403 | 0.89324 |
| | I10 | 0.91263 | 0.91849 | 0.91732 | 0.92418 | 0.92226 | 0.8431 | 0.9025 | **0.92624** |

Figure 4 summarizes the average SSIM values with different threshold levels. From Figure 4, we notice that the AEODE outperforms other algorithms, such as AEO, MPA, CS, GWO, GOA, and SSO, by achieving the highest average of SSIM with different threshold levels, with a slight advantage over MPA and SSO.

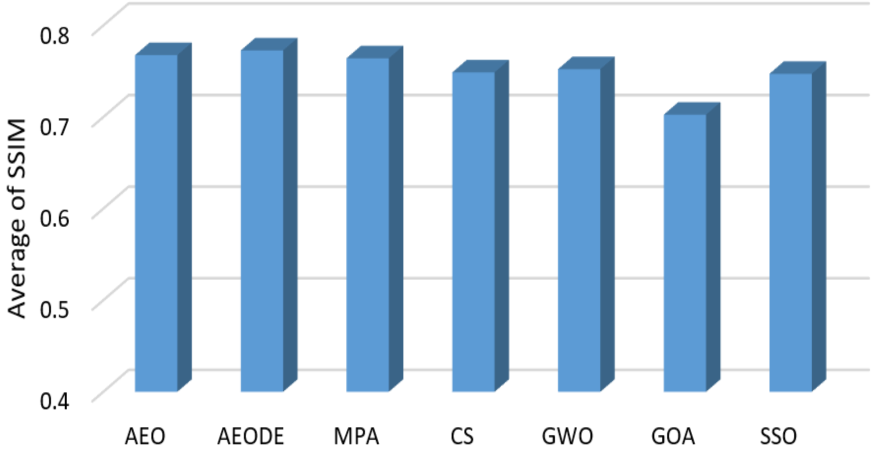

**Figure 4.** Average SSIM values for all algorithms' overall images.

### 5.2.2. Performance Measure by Peak Signal-to-Noise Ratio (PSNR)

Table 2 and Figure 5 present the performance of the AEODE, compared to other recent optimization algorithms based on PSNR measured with different threshold values.

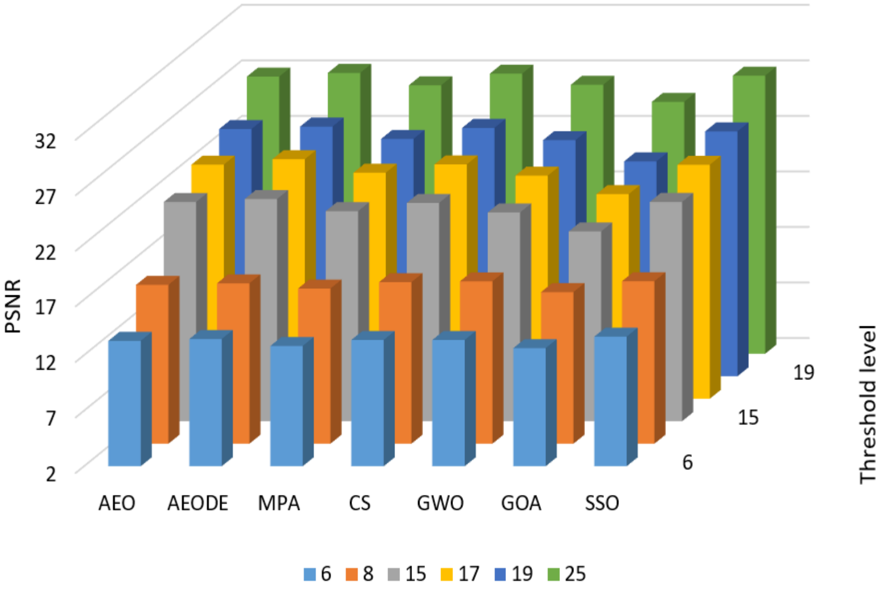

**Figure 5.** PSNR at different threshold levels.

It can be noticed from Figure 3 that the proposed AEODE outperforms other optimization algorithms at most threshold levels (except at level 8). Table 2 shows the PSNR values performed by the proposed method and other optimization algorithms for each image with all threshold levels.

**Table 2.** PSNR results for all algorithms (bold means the best value).

| Threshold | Image | AEO | AEODE | MPA | CS | GWO | GOA | SSO |
|---|---|---|---|---|---|---|---|---|
| 6 | I1 | 14.3825 | **14.8805** | 14.0022 | 14.2535 | 14.123 | 13.5623 | 14.5985 |
| | I2 | **16.776** | 16.5781 | 16.25 | 15.8815 | 15.6123 | 15.4548 | 15.9642 |
| | I3 | 10.301 | 10.4584 | 10.0393 | 12.8807 | 12.6054 | 11.3303 | **13.4835** |
| | I4 | 15.5356 | 15.6956 | 14.7613 | 16.2105 | **16.3312** | 16.0247 | 16.0098 |
| | I5 | 13.002 | **13.0219** | 12.7031 | 11.6661 | 11.9035 | 10.8805 | 12.5634 |
| | I6 | 13.8393 | **14.1526** | 13.4173 | 11.9244 | 12.183 | 11.5066 | 12.6031 |
| | I7 | 12.1668 | 12.2929 | 11.7442 | 11.983 | 11.8217 | 11.6867 | **12.3337** |
| | I8 | 13.8981 | 13.9791 | 13.5196 | **14.4894** | 14.0186 | 13.3968 | 14.1717 |
| | I9 | 11.5561 | **12.0803** | 11.0956 | 10.1514 | 10.5988 | 9.38632 | 10.1912 |
| | I10 | 11.394 | 11.3348 | 10.7158 | 14.212 | 14.4238 | 13.0733 | **14.7021** |
| 8 | I1 | 18.0812 | 18.0815 | 17.6837 | 18.1512 | 17.7062 | 17.0512 | **18.1623** |
| | I2 | 19.713 | 19.895 | **20.1166** | 16.8944 | 16.5392 | 15.6426 | 17.0666 |
| | I3 | 12.554 | 12.6388 | 11.8524 | 15.7199 | 15.9636 | 14.909 | **16.5606** |
| | I4 | 18.3923 | **18.567** | 18.5216 | 17.6977 | 17.0637 | 16.7765 | 17.7364 |
| | I5 | 16.5871 | **16.7741** | 16.2219 | 16.0126 | 16.1572 | 15.7477 | 15.7234 |
| | I6 | 17.726 | 17.9671 | **18.0062** | 15.1837 | 15.5847 | 14.0664 | 15.7411 |
| | I7 | 14.8103 | 14.9134 | 14.6142 | 15.9958 | 15.5439 | 15.1388 | **16.2394** |
| | I8 | 17.7434 | **18.0346** | 17.2219 | 15.1528 | 16.8989 | 14.7088 | 15.0617 |
| | I9 | 13.7439 | 13.7056 | 12.8298 | 15.5042 | 15.4239 | 14.2372 | **15.6629** |
| | I10 | 13.6444 | 13.8088 | 12.5811 | 19.1078 | **19.316** | 18.1821 | 18.3384 |
| 15 | I1 | 22.9214 | 22.977 | 22.2853 | **23.0132** | 21.5091 | 20.8354 | 22.8682 |
| | I2 | 23.5558 | **23.861** | 23.5189 | 22.437 | 22.187 | 20.0346 | 22.4572 |
| | I3 | 19.1193 | 19.4112 | 16.7735 | 21.5282 | 19.6672 | 19.2986 | **21.9266** |
| | I4 | 22.3949 | 22.249 | 22.0038 | 21.6674 | 21.6847 | 19.8822 | **22.5474** |
| | I5 | 21.7982 | **22.1718** | 21.3887 | 21.1647 | 21.2952 | 18.609 | 21.1493 |
| | I6 | **22.6571** | 22.4339 | 21.9557 | 21.1505 | 20.3099 | 17.7507 | 21.9507 |
| | I7 | 21.2712 | **22.3375** | 20.2573 | 21.3237 | 20.229 | 18.4218 | 21.5466 |
| | I8 | **22.219** | 22.1627 | 22.2886 | 21.8225 | 21.2988 | 18.7217 | 21.6013 |
| | I9 | 20.1963 | 20.8863 | 18.9355 | **20.9695** | 18.0963 | 17.7748 | 19.9499 |
| | I10 | 21.2212 | 21.558 | 19.7074 | 21.4588 | 21.4665 | 19.492 | 21.4161 |
| 17 | I1 | 24.0811 | 23.8706 | 23.5962 | **24.5295** | 23.0746 | 22.3151 | 24.2334 |
| | I2 | 24.7625 | **25.1301** | 24.5872 | 24.1457 | 24.0483 | 20.8547 | 23.8381 |
| | I3 | 20.8615 | 21.862 | 19.2265 | 23.327 | 20.6577 | 20.9033 | **23.3563** |
| | I4 | 22.9854 | **23.9083** | 23.2481 | 22.8942 | 22.4866 | 20.9846 | 22.8827 |
| | I5 | **23.4436** | 23.4242 | 22.3991 | 22.6849 | 22.8679 | 20.3653 | 22.2991 |
| | I6 | 23.6858 | 23.9178 | 23.1132 | 22.2126 | 22.1551 | 19.2307 | **23.9446** |
| | I7 | 23.0405 | **23.2971** | 21.5097 | 22.6135 | 21.4138 | 20.1451 | 22.1639 |
| | I8 | 23.5485 | **23.847** | 23.4845 | 22.6809 | 22.8869 | 19.9435 | 23.2374 |
| | I9 | 21.3322 | **22.7893** | 20.6068 | 22.7039 | 19.356 | 18.9158 | 21.635 |
| | I10 | 22.9969 | **23.5863** | 21.6966 | 23.1547 | 21.9301 | 20.5416 | 23.0256 |
| 19 | I1 | 24.4745 | 25.1133 | 24.517 | **25.2359** | 24.251 | 23.0769 | 25.1513 |
| | I2 | 25.6186 | 25.4214 | **25.5213** | 25.35 | 24.9708 | 22.2735 | 24.5691 |
| | I3 | 22.5205 | 23.8711 | 20.6197 | 24.743 | 21.7863 | 21.5832 | **25.1239** |
| | I4 | 24.6237 | **25.2183** | 24.561 | 23.7095 | 23.9133 | 21.4378 | 23.342 |
| | I5 | 24.2058 | **24.3305** | 23.3839 | 24.1541 | 23.8568 | 21.7525 | 23.1785 |
| | I6 | 24.6762 | 24.7183 | 24.4006 | **24.8508** | 23.6233 | 20.3269 | 24.0407 |
| | I7 | 23.6407 | 23.9977 | 23.3394 | **24.5317** | 22.6665 | 21.2738 | 24.2728 |
| | I8 | 23.8093 | **24.8603** | 24.0163 | 24.1517 | 23.8789 | 20.4655 | 24.1552 |
| | I9 | 24.225 | **22.7931** | 21.2062 | 22.5229 | 20.8636 | 19.7875 | 22.4684 |
| | I10 | **24.7213** | 24.4432 | 22.0929 | 24.3168 | 22.7555 | 21.4517 | 24.1257 |

**Table 2.** *Cont.*

| Threshold | Image | AEO | AEODE | MPA | CS | GWO | GOA | SSO |
|---|---|---|---|---|---|---|---|---|
| 25 | I1 | 26.9248 | **27.4147** | 26.7551 | 27.4008 | 26.7323 | 25.7589 | 27.4094 |
| | I2 | 27.912 | 28.2136 | 27.5864 | **28.2266** | 28.058 | 26.214 | 27.7472 |
| | I3 | 26.8428 | 27.1681 | 24.4243 | 26.8027 | 23.9304 | 23.9079 | **27.4464** |
| | I4 | 27.1151 | **27.5947** | 26.5531 | 26.7518 | 26.2573 | 24.955 | 26.3363 |
| | I5 | 26.8594 | 27.1087 | 26.1684 | **27.3946** | 26.9059 | 24.8264 | 26.3298 |
| | I6 | 27.1197 | 27.4133 | 26.8836 | 26.7446 | 27.1805 | 23.7763 | **28.3197** |
| | I7 | 26.7169 | 27.0784 | 25.6628 | **27.4061** | 25.9714 | 24.7308 | 26.7924 |
| | I8 | 27.1753 | **27.3743** | 26.6731 | 27.2032 | 26.7091 | 24.6398 | 26.6686 |
| | I9 | 25.9341 | 26.2033 | 24.8043 | **26.5647** | 24.4355 | 23.3068 | 25.7296 |
| | I10 | 26.8821 | 27.2701 | 26.1785 | **27.6637** | 25.9562 | 24.6613 | 27.6004 |

From Table 2, it is noticed that the proposed AEODE method allocates the first rank with the highest PSNR values at 23 cases, while SSO and CS are in second and third ranks with the highest 13 and 12 PSNR values, respectively. According to Table 2, the proposed AEODE method performs better with higher thresholding levels (at level 17 and higher) than lower levels.

Figure 6 summarizes the average PSNR values with all threshold levels. Figure 6 shows that our proposed method outperforms other optimization algorithms by achieving the highest average of PSNR with different threshold levels for all images. GOA achieves the worst performance, putting it last.

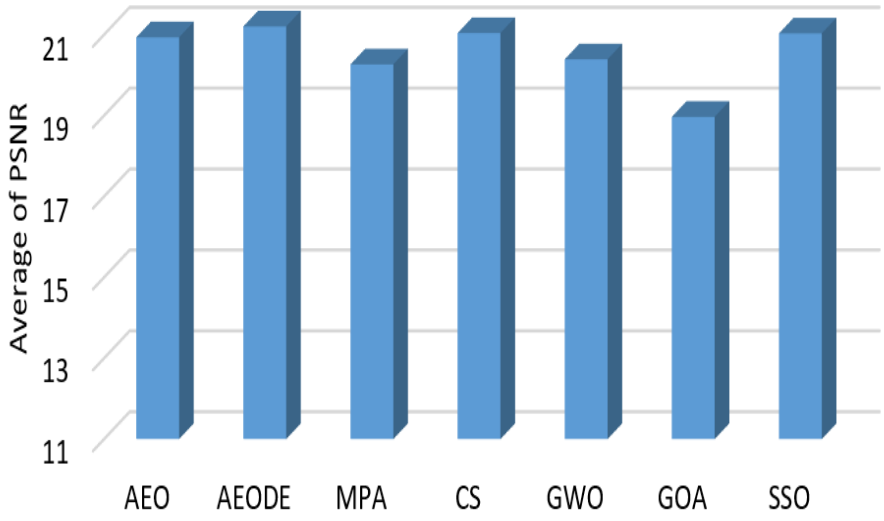

**Figure 6.** PSNR values of AEODE and other optimization algorithms.

### 5.2.3. Performance Measure by Fitness Function

Figure 7 and Table 3 show the fitness function values of AEODE method and other optimization algorithms with different threshold levels.

Based on Figure 7, the proposed AEODE method outperforms other optimization algorithms in all threshold levels, while GOA shows the lowest fitness values in all threshold levels.

Table 3 shows that all optimization algorithms achieve acceptable fitness values with all threshold levels. There is a slight advantage (in decimal levels) between each one. All optimization algorithms achieve higher fitness values along with higher thresholding levels. The higher the thresholding value, the better the fitness value obtained. Applying the 6, 8, 15, 17, 19, and 25 threshold levels achieves fitness values of 17, 20, 29, 32, 34, and 41, respectively. Figure 8 summarizes the average fitness values with all threshold levels.

Based on Figure 8, AEODE, MPA, and AEO came in the first, second, and third ranks, respectively, while GOA is ranked last.

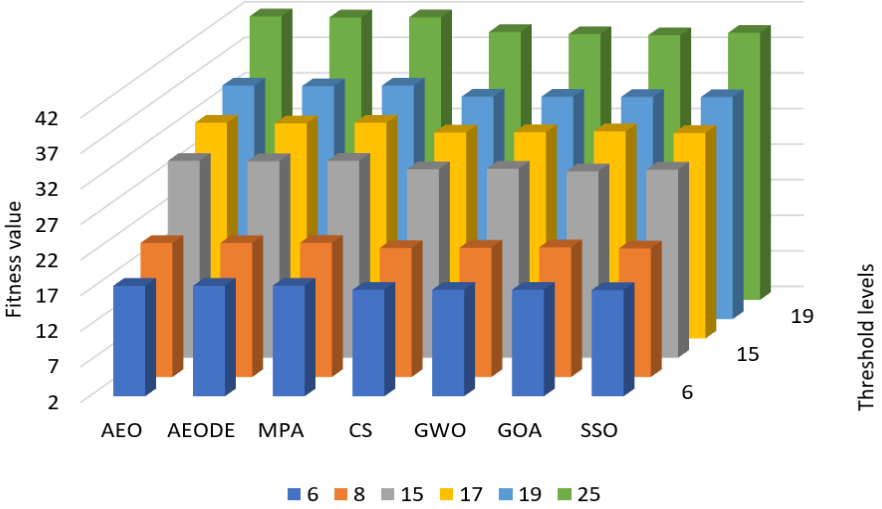

**Figure 7.** Fitness values of AEODE and other optimization algorithms.

**Table 3.** Fitness function results for all algorithms (bold means the best value).

| Threshold | Image | AEO | AEODE | MPA | CS | GWO | SSA | GOA | SSO |
|---|---|---|---|---|---|---|---|---|---|
| 6 | I1 | 17.5265 | 17.5167 | 17.5348 | 17.5163 | 17.5245 | 14.555 | **17.5398** | 17.4546 |
| | I2 | 17.5215 | 17.5209 | 17.5372 | 17.2918 | 17.2894 | 15.5694 | **17.3161** | 17.2726 |
| | I3 | 17.5249 | 17.52 | **17.5372** | 17.0874 | 17.0818 | 13.9699 | 17.1016 | 17.0616 |
| | I4 | 17.5298 | 17.5217 | 17.5364 | 17.5522 | 17.5704 | 15.3916 | **17.5896** | 17.5283 |
| | I5 | 17.5273 | 17.5211 | 17.5362 | **15.5982** | 15.5925 | 12.7276 | 15.6182 | 15.6395 |
| | I6 | 17.531 | 17.5214 | **17.5366** | 15.0703 | 15.0806 | 11.5213 | 15.1272 | 15.0172 |
| | I7 | 17.5305 | 17.5192 | 17.5379 | 17.6206 | **17.6236** | 15.135 | 17.3165 | 17.4764 |
| | I8 | 17.5323 | 17.5327 | 17.5334 | 17.5738 | **17.5903** | 15.4892 | **17.6009** | 17.5415 |
| | I9 | 17.5272 | 17.5201 | 17.5359 | 17.4772 | 17.5094 | 14.9546 | **17.5371** | 17.4722 |
| | I10 | 17.5233 | 17.5177 | **17.5364** | 16.7679 | 16.7749 | 14.0574 | 16.7988 | 16.7677 |
| 8 | I1 | 20.8258 | 20.8222 | **20.8474** | 20.7724 | 20.8195 | 15.6432 | **20.8393** | 20.6894 |
| | I2 | 20.8179 | 20.818 | 20.8467 | 20.7772 | 20.8182 | 16.2007 | **20.914** | 20.6923 |
| | I3 | 20.8335 | 20.8203 | 20.8516 | 20.443 | 20.4538 | 14.4673 | **20.5345** | 20.3825 |
| | I4 | 20.8315 | 20.8183 | 20.8546 | 20.9136 | 20.9509 | 16.3078 | **21.0092** | 20.8526 |
| | I5 | 20.8266 | 20.816 | **20.8484** | 18.2622 | 18.322 | 14.1362 | 18.3769 | 18.2611 |
| | I6 | 20.8341 | 20.8238 | **20.8486** | 17.3866 | 17.4261 | 11.5681 | 17.5021 | 17.2807 |
| | I7 | 20.8299 | 20.8306 | 20.8422 | 20.8701 | 20.9101 | 15.3929 | **20.9493** | 20.8268 |
| | I8 | 20.842 | 20.8136 | 20.8474 | 20.8738 | 20.8353 | 15.306 | **20.9881** | 20.8589 |
| | I9 | 20.8349 | 20.8287 | 20.8386 | 20.9832 | 21.0398 | 15.6711 | **21.0546** | 20.9873 |
| | I10 | 20.826 | 20.8282 | 20.8418 | 19.9763 | 20.0173 | 14.7812 | 20.0601 | 19.9178 |
| 15 | I1 | 29.6442 | 29.6133 | 29.6279 | 29.3907 | 29.4684 | 16.2101 | **29.8008** | 29.2784 |
| | I2 | 29.6674 | 29.6322 | 29.6724 | 29.6823 | **29.7556** | 16.0706 | 28.5566 | 29.6875 |
| | I3 | 29.6503 | 29.5867 | **29.5937** | 29.2606 | 29.2624 | 14.0884 | 28.5465 | 29.131 |
| | I4 | 29.6753 | 29.5881 | 29.6813 | 29.5308 | 29.6343 | 15.9021 | **30.0178** | 29.5538 |
| | I5 | 29.6461 | **29.6588** | 29.6368 | 25.204 | 25.2145 | 13.7662 | 25.7182 | 25.2165 |
| | I6 | **29.6671** | 29.6193 | 29.6527 | 23.6303 | 23.6167 | 11.6248 | 24.2313 | 23.1818 |
| | I7 | 29.6416 | 29.6049 | **29.6934** | 29.4742 | 29.5973 | 14.9086 | 28.6135 | 29.4155 |
| | I8 | 29.6577 | 29.6269 | 29.6843 | 30.0662 | **30.1392** | 15.5166 | 28.6444 | 30.0349 |
| | I9 | 29.6793 | 29.6249 | 29.6955 | 29.748 | **30.0096** | 15.2901 | 28.5204 | 29.9023 |
| | I10 | 29.6519 | 29.5961 | 29.6896 | 28.8684 | 28.9454 | 14.781 | **29.281** | 28.8635 |

**Table 3.** *Cont.*

| Threshold | Image | AEO | AEODE | MPA | CS | GWO | SSA | GOA | SSO |
|---|---|---|---|---|---|---|---|---|---|
| 17 | I1 | **32.3488** | 32.2296 | 32.3095 | 31.9577 | 31.9444 | 16.0424 | 31.0762 | 31.8416 |
| | I2 | 32.2875 | 32.2371 | 32.3061 | 32.3915 | 32.4331 | 15.7114 | **33.0069** | 32.4197 |
| | I3 | 32.3439 | 32.214 | 32.3012 | 31.7861 | 31.7911 | 15.0282 | **32.4284** | 31.6946 |
| | I4 | 32.2961 | 32.2027 | 32.2791 | 32.1339 | 32.1396 | 16.4578 | **32.7554** | 32.1749 |
| | I5 | 32.3251 | 32.2187 | **32.3283** | 27.1632 | 27.2144 | 13.1787 | 27.7373 | 27.2223 |
| | I6 | 32.3018 | 32.1828 | **32.2808** | 25.2824 | 25.287 | 11.5259 | 26.1223 | 24.6364 |
| | I7 | 32.2647 | 32.2341 | 32.3332 | 32.1072 | 32.1944 | 15.0693 | **32.6285** | 32.099 |
| | I8 | 32.3107 | 32.215 | 32.3415 | 32.6783 | 32.71 | 15.2613 | **33.3399** | 32.6571 |
| | I9 | 32.347 | 32.2675 | 32.2917 | 32.4441 | 32.5326 | 14.957 | 30.9936 | **32.4632** |
| | I10 | **32.3163** | 32.1987 | 32.3126 | 31.4601 | 31.5808 | 14.6868 | 31.0726 | 31.5033 |
| 19 | I1 | 34.8139 | 34.8003 | **34.8714** | 34.3638 | 34.2342 | 16.3417 | 33.2823 | 34.2175 |
| | I2 | 34.8117 | 34.7727 | 34.8053 | 34.9751 | 34.9733 | 16.3809 | 33.3096 | **35.0698** |
| | I3 | 34.8028 | 34.6484 | 34.7831 | 34.2196 | 34.14 | 14.9697 | **35.0649** | 34.0982 |
| | I4 | 34.8114 | 34.7633 | 34.8187 | 34.6671 | 34.6481 | 15.7964 | **35.3929** | 34.6825 |
| | I5 | **34.8495** | 34.7301 | 34.826 | 28.9961 | 29.036 | 13.6795 | 29.684 | 29.1493 |
| | I6 | **34.8331** | 34.7356 | 34.8254 | 26.7512 | 26.5405 | 11.5293 | 27.536 | 25.9821 |
| | I7 | 34.82 | 34.7292 | 34.8609 | 34.6364 | 34.73 | 15.3604 | **35.3216** | 34.5569 |
| | I8 | 34.808 | 34.7364 | 34.799 | 35.2033 | 35.228 | 15.4885 | **35.9805** | 35.2658 |
| | I9 | 34.8603 | 34.7427 | 34.8427 | 34.9619 | 35.0218 | 15.9977 | 33.319 | **35.0619** |
| | I10 | **34.8632** | 34.768 | 34.8505 | 33.9221 | 34.0155 | 15.1945 | 33.3191 | 34.0152 |
| 25 | I1 | **41.8453** | 41.7239 | 41.6587 | 41.0703 | 40.6435 | 17.1863 | 39.5637 | 40.9583 |
| | I2 | 41.8725 | 41.6996 | 41.7333 | 42.1871 | 41.8686 | 16.6713 | **42.9219** | 42.1336 |
| | I3 | 41.8546 | 41.756 | 41.7622 | 40.6073 | 40.2479 | 15.2268 | **41.681** | 40.417 |
| | I4 | 41.8022 | 41.6242 | 41.7986 | 41.5551 | 41.2241 | 17.3623 | **42.4607** | 41.6875 |
| | I5 | **41.8499** | 41.7091 | 41.724 | 33.8368 | 33.7225 | 14.7999 | 34.7461 | 33.9924 |
| | I6 | **41.8209** | 41.6941 | 41.7224 | 30.4701 | 29.6229 | 12.2152 | 32.0503 | 29.2935 |
| | I7 | **41.8718** | 41.7143 | 41.6714 | 41.5924 | 41.4857 | 16.0446 | 39.5462 | 41.5544 |
| | I8 | 41.8436 | 41.6505 | 41.671 | 42.3413 | 42.1102 | 16.375 | 39.7254 | **42.3516** |
| | I9 | 41.8299 | 41.632 | 41.6478 | 41.8899 | 41.9941 | 16.2916 | 39.5576 | **42.1339** |
| | I10 | **41.8737** | 41.7306 | 41.7884 | 40.8165 | 40.4964 | 15.9225 | 39.7665 | 40.7734 |

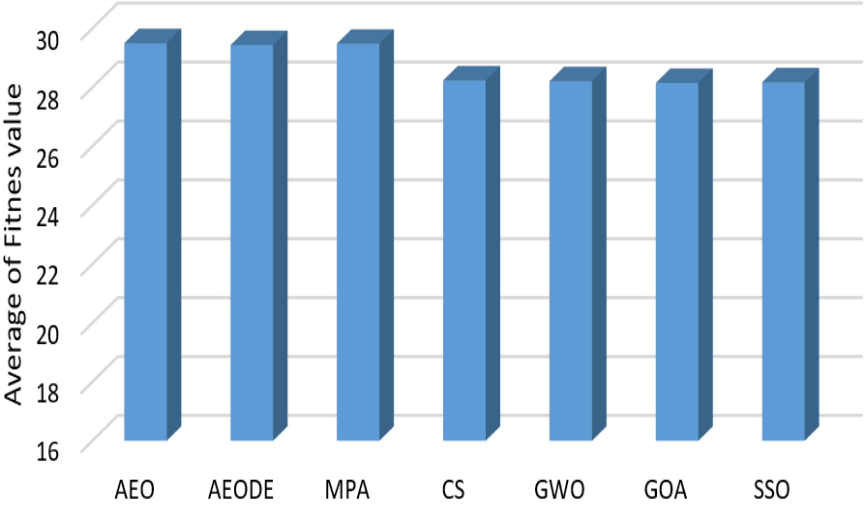

**Figure 8.** Average fitness values of AEODE and other optimization algorithms.

Figures 9 and 10 show the segmented image I10 and image I7, respectively, while their histograms at threshold value 19 are given in Figures 11 and 12 respectively. Both figures show that the proposed method has successfully determined the best threshold value to segment several types of images. Moreover, Figure 13 illustrates the quality of segmented image I1 at level 19. It can be noticed from this figure that the quality of AEODE is decreased in this case since its obtained threshold values do not cover the whole search space (as shown in Figure 14) and its feasible region does not contain the optimal threshold values, which affects the performance of the final output.

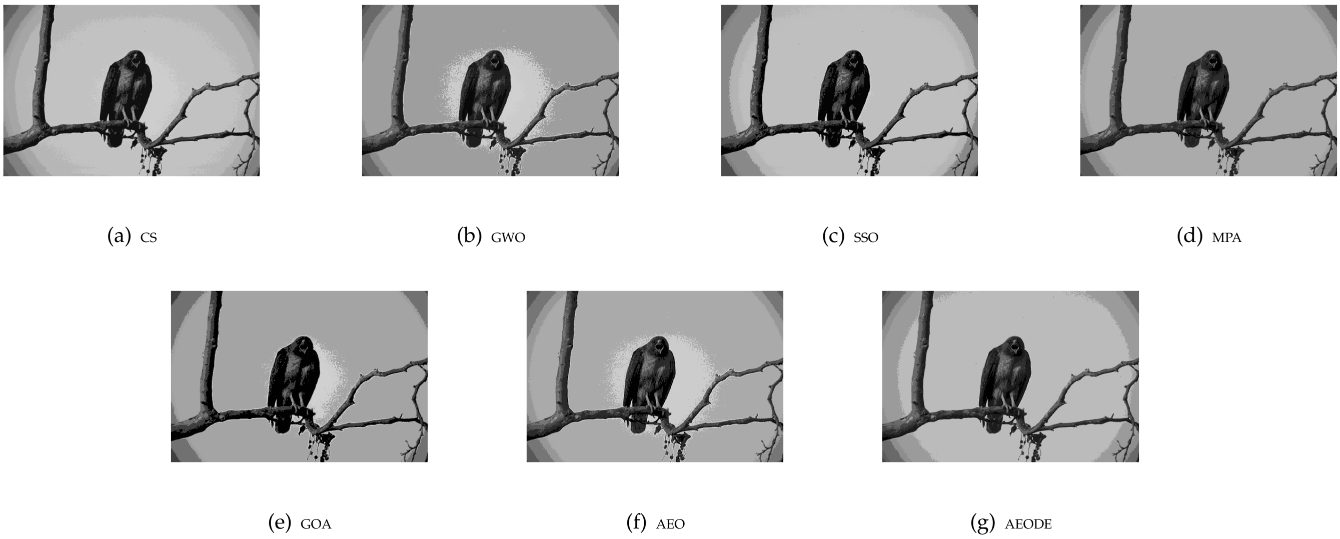
(a) CS (b) GWO (c) SSO (d) MPA (e) GOA (f) AEO (g) AEODE

**Figure 9.** Segmentation results at threshold level 19 for the images I10.

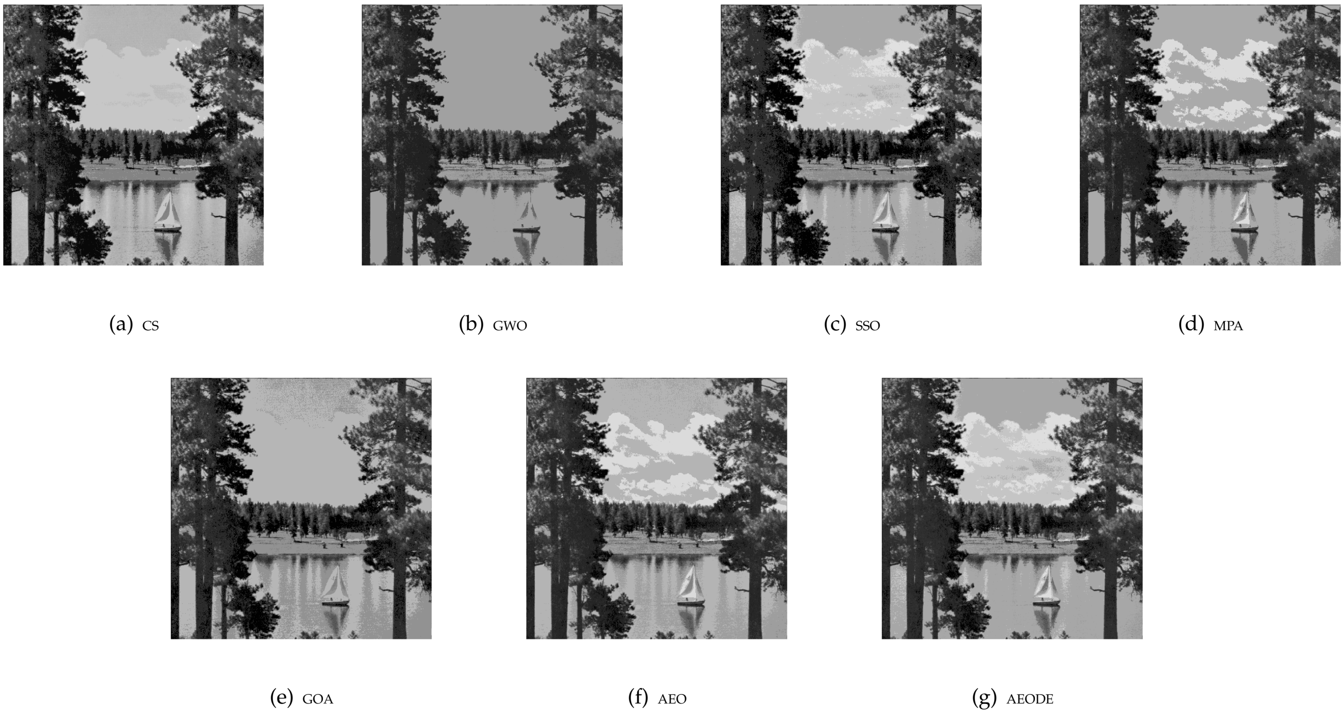
(a) CS (b) GWO (c) SSO (d) MPA (e) GOA (f) AEO (g) AEODE

**Figure 10.** Segmented image I7 at threshold level 19.

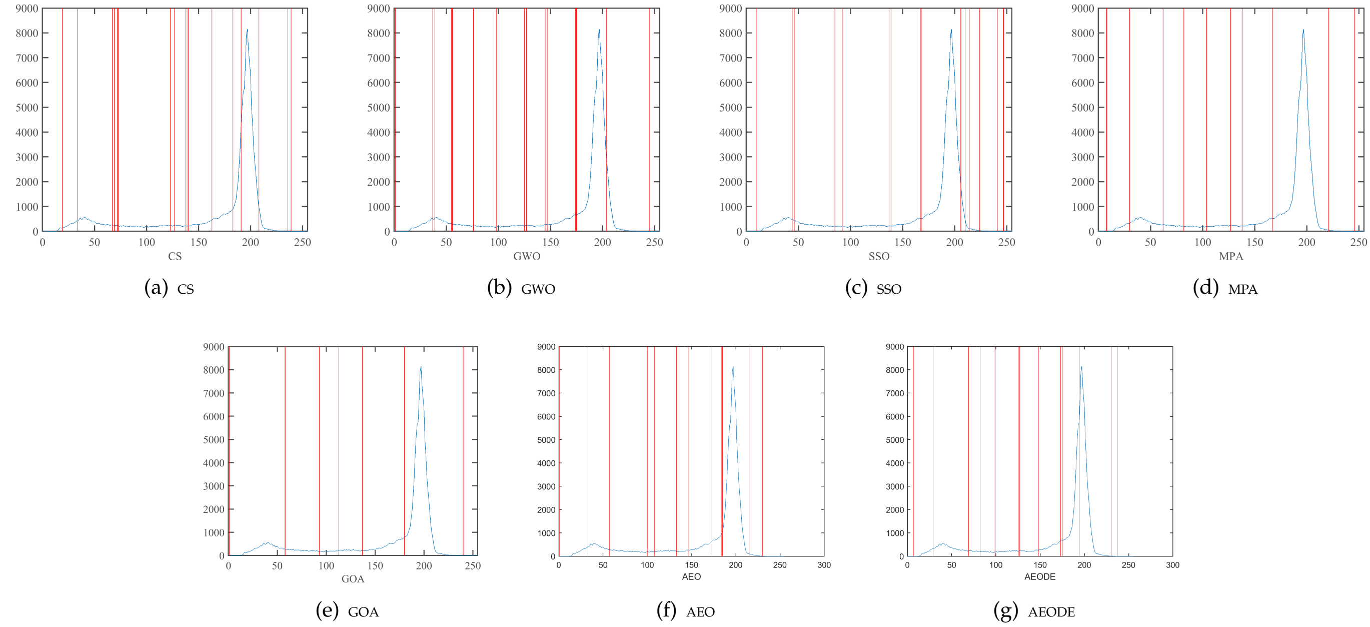

(a) CS (b) GWO (c) SSO (d) MPA

(e) GOA (f) AEO (g) AEODE

**Figure 11.** The threshold values at level 19 over the histogram of I10.

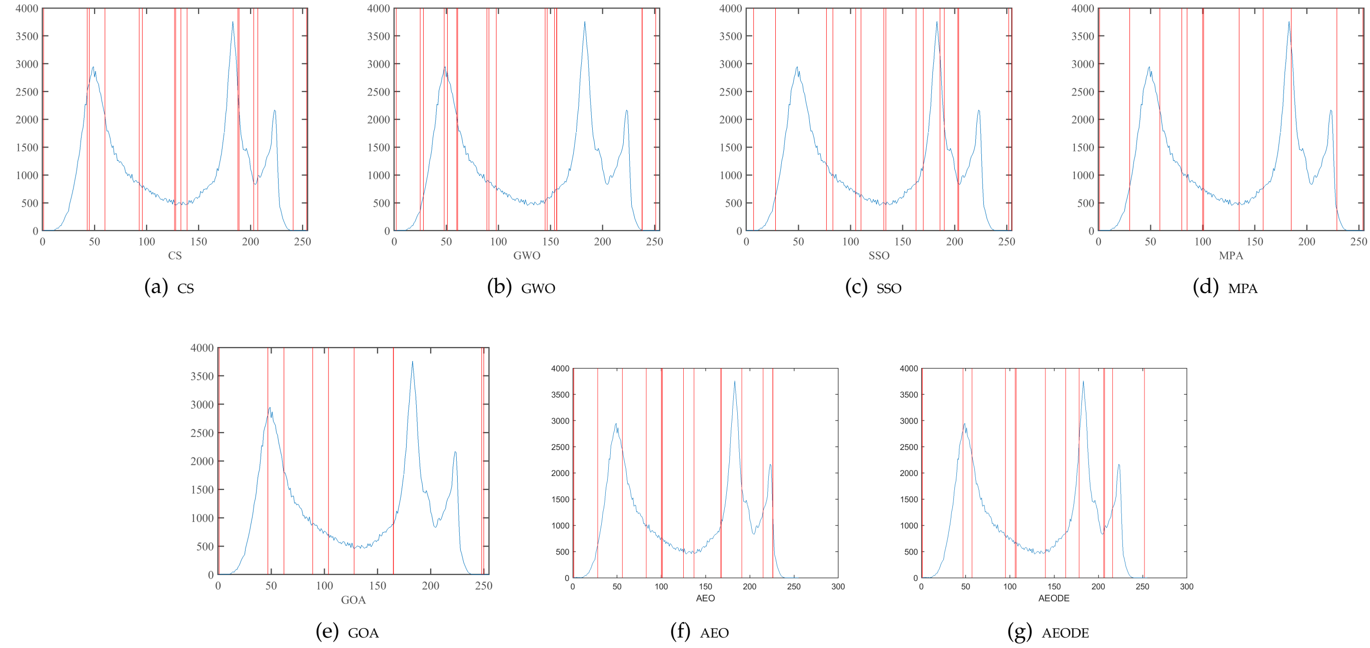

(a) CS (b) GWO (c) SSO (d) MPA

(e) GOA (f) AEO (g) AEODE

**Figure 12.** The threshold values at level 19 over the histogram of image I7.

Moreover, the improvement rate between the proposed method and other methods according to each performance measure is computed as follows:

$$IR(\%) = \frac{(S - S')}{S'} * 100 \tag{35}$$

where $S'$ and $S$ denote the values obtained by AEODE and values obtained by other methods, respectively.

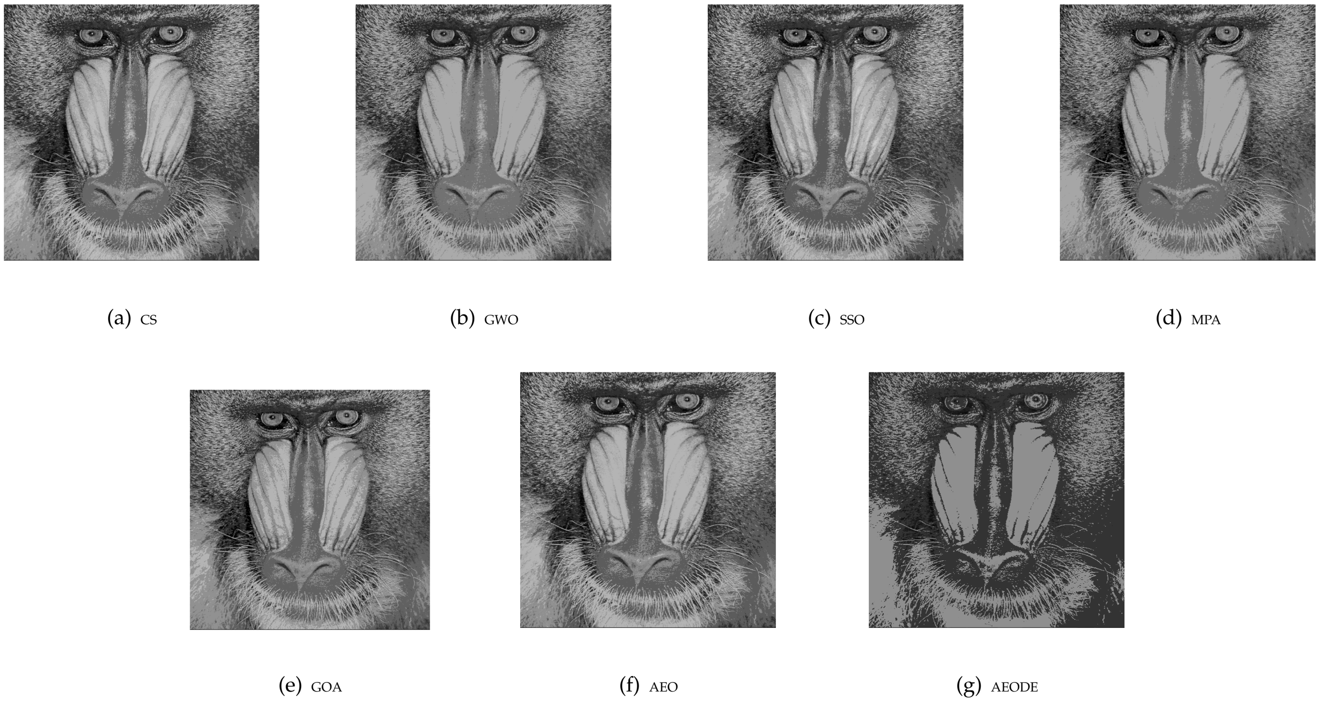
(a) CS (b) GWO (c) SSO (d) MPA (e) GOA (f) AEO (g) AEODE

**Figure 13.** Segmented image I1 at threshold level 19.

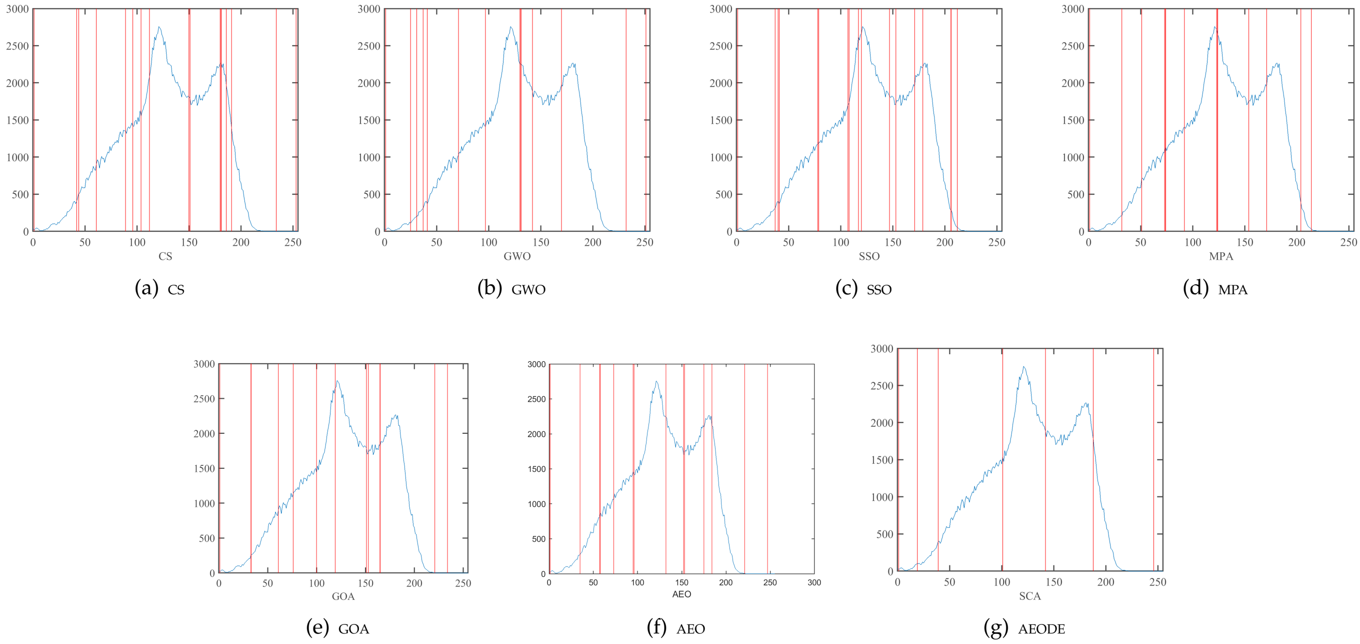

(a) CS (b) GWO (c) SSO (d) MPA (e) GOA (f) AEO (g) AEODE

**Figure 14.** The threshold values at level 19 over the histogram of image I1.

Table 4 shows the IR for the three measures (i.e., PSNR, SSIM, and fitness value). From this table, it can be noticed that AEODE provides a high IR rate in terms of PSNR, which is better than AEO, MPA, CS, GWO, GOA, and SSO with 47, 46, 44, 44, 55, and 46. In terms of SSIM as well, it provides results better than AEO, MPA, CS, GWO, GOA, and SSO with 49, 56, 37, 51, 53, and 39. However, the IR of the developed AEODE in terms of the fitness value is better than AEO and MPA with only 5 and 3 cases. However, with other methods, it still provides better fitness values of 41, 37, 37, and 42 for CS, GWO, GOA, and SSO.

**Table 4.** Improvement ratio for developed method with other methods (bold means the best value).

| | | **PSNR** | | | | | | **SSIM** | | | | | | **Fitness** | | | | | |
|---|---|---|---|---|---|---|---|---|---|---|---|---|---|---|---|---|---|---|---|
| **T** | **I** | **AEO** | **MPA** | **CS** | **GWO** | **GOA** | **SSO** | **AEO** | **MPA** | **CS** | **GWO** | **GOA** | **SSO** | **AEO** | **MPA** | **CS** | **GWO** | **GOA** | **SSO** |
| 6 | I1 | **−5.0** | **−10.0** | **−6.8** | **−9.2** | **−12.8** | **−4.0** | **−3.3** | **−5.9** | **−4.2** | **−5.1** | **−8.9** | **−1.9** | 0.1 | 0.1 | **−0.0** | 0.0 | 0.1 | **−0.4** |
| | I2 | 1.9 | **−3.5** | **−7.0** | **−7.4** | **−11.4** | **−5.9** | 1.2 | **−2.0** | **−4.2** | **−5.8** | **−6.8** | **−3.7** | 0.0 | 0.1 | **−1.3** | **−1.3** | **−1.2** | **−1.4** |
| | I3 | **−1.4** | **−3.8** | **−0.9** | **−2.4** | **−1.5** | 2.4 | **−1.5** | **−4.0** | 23.2 | 20.5 | 8.3 | 28.9 | 0.0 | 0.1 | **−2.5** | **−2.5** | **−2.4** | **−2.6** |
| | I4 | **−1.7** | **−8.7** | 2.9 | 4.1 | 1.7 | 1.0 | **−1.0** | **−6.0** | 3.3 | 4.0 | 2.1 | 2.0 | 0.0 | 0.1 | 0.2 | 0.3 | 0.4 | 0.0 |
| | I5 | **−1.2** | **−5.9** | **−25.2** | **−21.3** | **−38.3** | **−11.2** | **−0.2** | **−2.4** | **−10.4** | **−8.6** | **−16.4** | **−3.5** | 0.0 | 0.1 | **−11.0** | **−11.0** | **−10.9** | **−10.7** |
| | I6 | **−4.1** | **−9.1** | **−25.6** | **−21.2** | **−32.8** | **−16.3** | **−2.2** | **−5.2** | **−15.7** | **−13.9** | **−18.7** | **−10.9** | 0.1 | 0.1 | **−14.0** | **−13.9** | **−13.7** | **−14.3** |
| | I7 | **−2.0** | **−7.1** | **−9.3** | **−9.4** | **−14.4** | **−7.0** | **−1.0** | **−4.5** | **−2.5** | **−3.8** | **−4.9** | 0.3 | 0.1 | 0.1 | 0.6 | 0.6 | **−1.2** | **−0.2** |
| | I8 | **−0.9** | **−3.7** | 4.6 | 1.2 | **−4.4** | 2.3 | **−0.6** | **−3.3** | 3.7 | 0.3 | **−4.2** | 1.4 | **−0.0** | 0.0 | 0.2 | 0.3 | 0.4 | 0.1 |
| | I9 | **−1.3** | **−2.0** | **−21.2** | **−4.3** | **−23.1** | **−25.9** | **−4.3** | **−8.2** | **−16.0** | **−12.3** | **−22.3** | **−15.6** | 0.0 | 0.1 | **−0.2** | **−0.1** | 0.1 | **−0.3** |
| | I10 | 0.4 | **−3.3** | **−12.5** | **−12.4** | **−16.9** | **−9.5** | 0.5 | **−5.5** | 25.4 | 27.3 | 15.3 | 29.7 | 0.0 | 0.1 | **−4.3** | **−4.2** | **−4.1** | **−4.3** |
| 8 | I1 | 0.8 | **−1.4** | **−0.8** | **−2.3** | **−5.6** | **−2.1** | **−0.0** | **−2.2** | 0.4 | **−2.1** | **−5.7** | 0.4 | 0.0 | 0.1 | **−0.2** | **−0.0** | 0.1 | **−0.6** |
| | I2 | **−2.8** | 3.1 | **−20.2** | **−19.7** | **−29.0** | **−18.4** | **−0.9** | 1.1 | **−15.1** | **−16.9** | **−21.4** | **−14.2** | **−0.0** | 0.1 | **−0.2** | 0.0 | 0.5 | **−0.6** |
| | I3 | 0.2 | **−2.9** | 5.4 | 4.3 | 4.2 | 7.5 | **−0.7** | **−6.2** | 24.4 | 26.3 | 18.0 | 31.0 | 0.1 | 0.2 | **−1.8** | **−1.8** | **−1.4** | **−2.1** |
| | I4 | **−1.1** | 1.0 | **−7.9** | **−9.7** | **−12.1** | **−7.3** | **−0.9** | **−0.2** | **−4.7** | **−8.1** | **−9.6** | **−4.5** | 0.1 | 0.2 | 0.5 | 0.6 | 0.9 | 0.2 |
| | I5 | **−0.6** | 0.2 | **−12.9** | **−10.9** | **−15.4** | **−15.8** | **−1.1** | **−3.3** | **−4.5** | **−3.7** | **−6.1** | **−6.3** | 0.1 | 0.2 | **−12.3** | **−12.0** | **−11.7** | **−12.3** |
| | I6 | **−0.4** | 1.9 | **−19.5** | **−15.9** | **−29.8** | **−16.2** | **−1.3** | 0.2 | **−15.5** | **−13.3** | **−21.7** | **−12.4** | 0.0 | 0.1 | **−16.5** | **−16.3** | **−16.0** | **−17.0** |
| | I7 | **−0.4** | 3.5 | **−5.1** | **−7.7** | **−12.9** | **−4.3** | **−0.7** | **−2.0** | 7.3 | 4.2 | 1.5 | 8.9 | **−0.0** | 0.1 | 0.2 | 0.4 | 0.6 | **−0.0** |
| | I8 | **−1.3** | **−2.6** | **−11.8** | **−3.7** | **−13.3** | **−13.7** | **−1.6** | **−4.5** | **−16.0** | **−6.3** | **−18.4** | **−16.5** | 0.1 | 0.2 | 0.3 | 0.1 | 0.8 | 0.2 |
| | I9 | 0.6 | 0.6 | 5.0 | 4.8 | 1.7 | 5.0 | 0.3 | **−6.4** | 13.1 | 12.5 | 3.9 | 14.3 | 0.0 | 0.0 | 0.7 | 1.0 | 1.1 | 0.8 |
| | I10 | **−0.2** | **−2.2** | **−7.3** | **−8.9** | **−11.9** | **−8.1** | **−1.2** | **−8.9** | 38.4 | 39.9 | 31.7 | 32.8 | **−0.0** | 0.1 | **−4.1** | **−3.9** | **−3.7** | **−4.4** |
| 15 | I1 | **−0.1** | **−1.0** | **−0.7** | **−3.6** | **−5.7** | **−0.9** | **−0.2** | **−3.0** | 0.2 | **−6.4** | **−9.3** | **−0.5** | 0.1 | 0.0 | **−0.8** | **−0.5** | 0.6 | **−1.1** |
| | I2 | **−2.7** | **−0.7** | **−7.3** | **−3.3** | **−19.4** | **−8.7** | **−1.3** | **−1.4** | **−6.0** | **−7.0** | **−16.0** | **−5.9** | 0.1 | 0.1 | 0.2 | 0.4 | **−3.6** | 0.2 |
| | I3 | **−0.4** | **−4.7** | 3.1 | 2.5 | **−0.3** | 2.1 | **−1.5** | **−13.6** | 10.9 | 1.3 | **−0.6** | 13.0 | 0.2 | 0.0 | **−1.1** | **−1.1** | **−3.5** | **−1.5** |
| | I4 | 0.6 | **−0.0** | **−3.0** | **−1.8** | **−10.7** | **−0.2** | 0.7 | **−1.1** | **−2.6** | **−2.5** | **−10.6** | 1.3 | 0.3 | 0.3 | **−0.2** | 0.2 | 1.5 | **−0.1** |
| | I5 | **−1.0** | **−1.4** | **−5.7** | **−3.0** | **−16.8** | **−5.7** | **−1.7** | **−3.5** | **−4.5** | **−4.0** | **−16.1** | **−4.6** | **−0.0** | **−0.1** | **−15.0** | **−15.0** | **−13.3** | **−15.0** |
| | I6 | 0.6 | **−0.9** | **−3.0** | **−5.5** | **−19.2** | **−1.1** | 1.0 | **−2.1** | **−5.7** | **−9.5** | **−20.9** | **−2.2** | 0.2 | 0.1 | **−20.2** | **−20.3** | **−18.2** | **−21.7** |
| | I7 | **−0.2** | 2.0 | **−0.4** | 2.9 | **−16.2** | **−0.9** | **−4.8** | **−9.3** | **−4.5** | **−9.4** | **−17.5** | **−3.5** | 0.1 | 0.3 | **−0.4** | **−0.0** | **−3.3** | **−0.6** |
| | I8 | 0.9 | 1.5 | **−1.3** | **−0.0** | **−8.3** | **−1.1** | 0.3 | 0.6 | **−1.5** | **−3.9** | **−15.5** | **−2.5** | 0.1 | 0.2 | 1.5 | 1.7 | **−3.3** | 1.4 |
| | I9 | **−1.0** | **−0.8** | **−3.0** | **−2.4** | **−5.7** | **−4.9** | **−3.3** | **−9.3** | 0.4 | **−13.4** | **−14.9** | **−4.5** | 0.2 | 0.2 | 0.4 | 1.3 | **−3.7** | 0.9 |
| | I10 | **−0.6** | 0.1 | **−5.7** | **−7.5** | **−10.0** | **−7.6** | **−1.6** | **−8.6** | **−0.5** | **−0.4** | **−9.6** | **−0.7** | 0.2 | 0.3 | **−2.5** | **−2.2** | **−1.1** | **−2.5** |

**Table 4.** *Cont.*

| | | PSNR | | | | | | SSIM | | | | | | Fitness | | | | | |
|---|---|---|---|---|---|---|---|---|---|---|---|---|---|---|---|---|---|---|---|
| **T** | **I** | **AEO** | **MPA** | **CS** | **GWO** | **GOA** | **SSO** | **AEO** | **MPA** | **CS** | **GWO** | **GOA** | **SSO** | **AEO** | **MPA** | **CS** | **GWO** | **GOA** | **SSO** |
| 17 | I1 | 0.7 | **−0.7** | 1.0 | **−2.3** | **−3.7** | 0.1 | 0.9 | **−1.1** | 2.8 | **−3.3** | **−6.5** | 1.5 | 0.4 | 0.2 | **−0.8** | **−0.9** | **−3.6** | **−1.2** |
| | I2 | **−1.9** | **−0.9** | **−3.7** | **−0.8** | **−19.3** | **−5.5** | **−1.5** | **−2.2** | **−3.9** | **−4.3** | **−17.0** | **−5.1** | 0.2 | 0.2 | 0.5 | 0.6 | 2.4 | 0.6 |
| | I3 | 1.7 | **−0.7** | 4.3 | 4.1 | 2.1 | 4.7 | **−4.6** | **−12.1** | 6.7 | **−5.5** | **−4.4** | 6.8 | 0.4 | 0.3 | **−1.3** | **−1.3** | 0.7 | **−1.6** |
| | I4 | **−2.8** | **−1.3** | **−3.7** | **−3.9** | **−9.6** | **−3.9** | **−3.9** | **−2.8** | **−4.2** | **−5.9** | **−12.2** | **−4.3** | 0.3 | 0.2 | **−0.2** | **−0.2** | 1.7 | **−0.1** |
| | I5 | **−0.5** | **−1.1** | **−3.8** | **−1.7** | **−11.5** | **−4.8** | 0.1 | **−4.4** | **−3.2** | **−2.4** | **−13.1** | **−4.8** | 0.3 | 0.3 | **−15.7** | **−15.5** | **−13.9** | **−15.5** |
| | I6 | **−0.4** | **−1.2** | **−2.3** | **−2.6** | **−14.9** | 1.2 | **−1.0** | **−3.4** | **−7.1** | **−7.4** | **−19.6** | 0.1 | 0.4 | 0.3 | **−21.4** | **−21.4** | **−18.8** | **−23.4** |
| | I7 | **−1.1** | **−1.9** | **−3.3** | 0.6 | **−10.5** | **−4.1** | **−1.1** | **−7.7** | **−2.9** | **−8.1** | **−13.5** | **−4.9** | 0.1 | 0.3 | **−0.4** | **−0.1** | 1.2 | **−0.4** |
| | I8 | **−0.4** | **−0.1** | **−3.4** | **−0.9** | **−9.1** | **−2.3** | **−1.3** | **−1.5** | **−4.9** | **−4.0** | **−16.4** | **−2.6** | 0.3 | 0.4 | 1.4 | 1.5 | 3.5 | 1.4 |
| | I9 | **−0.5** | **−0.1** | **−1.7** | **−2.2** | **−4.9** | **−2.2** | **−6.4** | **−9.6** | **−0.4** | **−15.1** | **−17.0** | **−5.1** | 0.2 | 0.1 | 0.5 | 0.8 | **−3.9** | 0.6 |
| | I10 | 0.5 | 1.0 | **−3.2** | **−6.5** | **−6.7** | **−4.0** | **−2.5** | **−8.0** | **−1.8** | **−7.0** | **−12.9** | **−2.4** | 0.4 | 0.4 | **−2.3** | **−1.9** | **−3.5** | **−2.2** |
| 19 | I1 | **−1.0** | **−1.0** | **−0.2** | **−2.2** | **−4.2** | **−0.5** | **−2.5** | **−2.4** | 0.5 | **−3.4** | **−8.1** | 0.2 | 0.0 | 0.2 | **−1.3** | **−1.6** | **−4.4** | **−1.7** |
| | I2 | **−1.4** | 0.2 | **−2.0** | 1.1 | **−14.3** | **−4.9** | 0.8 | 0.4 | **−0.3** | **−1.8** | **−12.4** | **−3.4** | 0.1 | 0.1 | 0.6 | 0.6 | **−4.2** | 0.9 |
| | I3 | 0.8 | **−0.6** | 3.8 | 3.6 | 1.7 | 4.3 | **−5.7** | **−13.6** | 3.7 | **−8.7** | **−9.6** | 5.2 | 0.4 | 0.4 | **−1.2** | **−1.5** | 1.2 | **−1.6** |
| | I4 | **−1.6** | **−0.8** | **−4.5** | **−3.4** | **−11.6** | **−5.4** | **−2.4** | **−2.6** | **−6.0** | **−5.2** | **−15.0** | **−7.4** | 0.1 | 0.2 | **−0.3** | **−0.3** | 1.8 | **−0.2** |
| | I5 | **−0.4** | **−2.5** | **−1.7** | **−1.5** | **−9.0** | **−4.7** | **−0.5** | **−3.9** | **−0.7** | **−1.9** | **−10.6** | **−4.7** | 0.3 | 0.3 | **−16.5** | **−16.4** | **−14.5** | **−16.1** |
| | I6 | 0.1 | 0.2 | 2.8 | **−0.5** | **−12.1** | 0.2 | **−0.2** | **−1.3** | 0.5 | **−4.4** | **−17.8** | **−2.7** | 0.3 | 0.3 | **−23.0** | **−23.6** | **−20.7** | **−25.2** |
| | I7 | **−0.5** | 0.7 | 1.2 | 1.9 | **−7.6** | **−0.5** | **−1.5** | **−2.7** | 2.2 | **−5.5** | **−11.4** | 1.1 | 0.3 | 0.4 | **−0.3** | 0.0 | 1.7 | **−0.5** |
| | I8 | **−1.5** | **−1.0** | **−1.2** | **−0.7** | **−9.1** | **−2.0** | **−4.2** | **−3.4** | **−2.9** | **−3.9** | **−17.7** | **−2.8** | 0.2 | 0.2 | 1.3 | 1.4 | 3.6 | 1.5 |
| | I9 | **−0.3** | **−0.5** | **−1.9** | **−1.8** | **−5.7** | **−2.0** | 6.3 | **−7.0** | **−1.2** | **−8.5** | **−13.2** | **−1.4** | 0.3 | 0.3 | 0.6 | 0.8 | **−4.1** | 0.9 |
| | I10 | **−1.0** | 1.3 | **−1.2** | **−3.2** | **−5.0** | **−4.1** | 1.1 | **−9.6** | **−0.5** | **−6.9** | **−12.2** | **−1.3** | 0.3 | 0.2 | **−2.4** | **−2.2** | **−4.2** | **−2.2** |
| 25 | I1 | **−0.7** | **−0.8** | **−0.3** | **−1.3** | **−2.5** | **−0.4** | **−1.8** | **−2.4** | **−0.1** | **−2.5** | **−6.0** | **−0.0** | 0.3 | **−0.2** | **−1.6** | **−2.6** | **−5.2** | **−1.8** |
| | I2 | **−0.7** | **−0.9** | 0.7 | 4.0 | **−4.7** | **−1.4** | **−1.1** | **−2.2** | 0.0 | **−0.6** | **−7.1** | **−1.7** | 0.4 | 0.1 | 1.2 | 0.4 | 2.9 | 1.0 |
| | I3 | **−1.8** | **−0.0** | 2.4 | 2.0 | **−0.0** | 1.7 | **−1.2** | **−10.1** | **−1.3** | **−11.9** | **−12.0** | 1.0 | 0.2 | 0.0 | **−2.8** | **−3.6** | **−0.2** | **−3.2** |
| | I4 | **−0.7** | **−1.9** | **−1.7** | **−2.4** | **−6.1** | **−2.7** | **−1.7** | **−3.8** | **−3.1** | **−4.8** | **−9.6** | **−4.6** | 0.4 | 0.4 | **−0.2** | **−1.0** | 2.0 | 0.2 |
| | I5 | **−0.3** | **−0.9** | 0.0 | **−0.1** | **−5.0** | **−2.0** | **−0.9** | **−3.5** | 1.1 | **−0.7** | **−8.4** | **−2.9** | 0.3 | 0.0 | **−18.9** | **−19.1** | **−16.7** | **−18.5** |
| | I6 | **−0.7** | **−0.8** | 0.4 | 1.7 | **−5.7** | 2.3 | **−1.1** | **−1.9** | **−2.4** | **−0.8** | **−13.3** | 3.3 | 0.3 | 0.1 | **−26.9** | **−29.0** | **−23.1** | **−29.7** |
| | I7 | **−0.7** | **−1.0** | 0.6 | 0.3 | **−3.5** | **−0.5** | **−1.3** | **−5.2** | 1.2 | **−4.1** | **−8.7** | **−1.1** | 0.4 | **−0.1** | **−0.3** | **−0.5** | **−5.2** | **−0.4** |
| | I8 | **−0.5** | **−0.6** | **−0.9** | **−0.6** | **−3.9** | **−1.7** | **−0.7** | **−2.6** | **−0.6** | **−2.4** | **−10.0** | **−2.6** | 0.5 | 0.0 | 1.7 | 1.1 | **−4.6** | 1.7 |
| | I9 | **−0.7** | **−0.7** | **−0.5** | **−1.6** | **−3.8** | **−1.6** | **−1.0** | **−5.3** | 1.4 | **−6.7** | **−11.1** | **−1.8** | 0.5 | 0.0 | 0.6 | 0.9 | **−5.0** | 1.2 |
| | I10 | **−0.6** | **−0.1** | 0.6 | 0.4 | **−1.7** | 0.8 | **−1.4** | **−4.0** | 1.4 | **−4.8** | **−9.6** | 1.2 | 0.3 | 0.1 | **−2.2** | **−3.0** | **−4.7** | **−2.3** |

T in first column is the threshold level. I is the image name.

### 5.3. Statistical Results

In this section, we apply the Friedman test to evaluate the robustness of the algorithms based on all measures. This test statistically ranks the methods, where the highest Friedman's value is the best.

From Table 5, it can be seen that the AEODE achieved the highest mean rank compared to all methods in both SSIM and PSNR measures, followed by AEO, MPA, CS, and GWO, respectively, where the GOA ranked last in the PSNR measure. In the SSIM measure, the AEO, CS, and SSO ranked second, third, and fourth, respectively, followed by MPA and GWO. The GOA also came in last. However, the AEODE obtained the best values in the PSNR and SSIM measure, and it achieved the fourth rank after AEO, MPA, and GOA in the fitness function measure. This can be due to the fact that the fitness function did not measure the quality of the image like the other two measures. Therefore, we can conclude that the AEODE can effectively segment images better than the compared methods.

**Table 5.** Results of the Friedman test for all measures (bold means the best value).

| | **AEODE** | **AEO** | **MPA** | **CS** | **GWO** | **SSA** | **GOA** | **SSO** |
|---|---|---|---|---|---|---|---|---|
| SSIM | **6.617** | 5.617 | 5.267 | 5.017 | 4.742 | 2.083 | 2.183 | 4.475 |
| PSNR | **5.750** | 4.700 | 3.350 | 4.783 | 3.300 | 1.100 | 1.483 | 4.633 |
| Fitness | 4.750 | 6.100 | **6.267** | 4.233 | 4.633 | 1.000 | 5.217 | 3.800 |

The proposed AEODE achieved higher performance in both measures, SSIM and PSNR, for most threshold levels, whereas it obtained good results in terms of fitness values. It outperformed the basic version of AEO, as it combines and reserves the best features for each of AEO and DE. It also shows advantages in SSIM, PSNR, and fitness values, compared to other optimization algorithms, such as MPA, CS, GWO, SSO, and GOA, which means high efficiency of exploring problem space. The proposed method achieves two main tasks; avoiding stacking at a local point (and consequently being trapped) and increasing the convergence ability. We believe that achieving acceptable performance with a small (compared to other algorithms) number of parameters, which imply a relatively simple implementation task, is considered a great advantage. The hybridization of swarm algorithms is aligned with other literature, as they showed advantages toward solving complex problems, such as determining an optimal threshold value for image segmentation.

## 6. Conclusions and Future Work

The segmentation process is the primary step in the image processing field, as it is employed in different computer vision applications. Multilevel thresholding techniques have confirmed their efficiency in solving image segmentation problems. This paper presents a new multilevel thresholding method based on a modified artificial ecosystem-based optimization (AEO) algorithm, using differential evolution (DE), called AEODE. The AEO is a recently proposed optimization algorithm inspired by the chain of energy transfer among living organisms, and it was successfully applied to address various optimization problems. However, it suffers from some limitations, such as stacking at the local optima. Therefore, in this paper, the DE was employed to overcome the drawbacks of the AEO. It was applied as a local search for the AEO to improve the ecosystem of the solutions. A set of images was applied to evaluate the performance of the AEODE using three measures, namely structural similarity index (SSIM), peak signal-to-noise ratio (PSNR), and fitness function values. The AEODE was compared with seven well-known optimization algorithms, including the traditional AEO, gray wolf optimization (GWO), marine predators algorithm (MPA), spherical search optimization (SSO), grasshopper optimization algorithm (GOA), and cuckoo search (CS) algorithm. The evaluation outcomes confirmed the competitive performance of the proposed AEODE, which outperformed the traditional AEO and other compared algorithms on different tests. Furthermore, to evaluate the robustness of the AEODE method and the compared algorithms, we applied a well-known statistical test, called the Friedman test. The AEODE obtained the highest mean rank.

In future work, the proposed AEODE can be applied in different optimization applications, such as parameter estimation, feature selection, and data clustering. Moreover, other recent optimizers can be applied to find alternative solutions to the multilevel thresholding image segmentation problem, such as the arithmetic optimization algorithm (AOA).

**Author Contributions:** A.A.E.: Conceptualization, supervision, methodology, formal analysis, resources, data curation, and writing—original draft preparation. L.A.: Conceptualization, supervision, methodology, formal analysis, resources, data curation, and writing—original draft preparation. D.Y.: Writing—review and editing. A.T.S.: Writing—review and editing. M.A.A.A.-q.: Writing—review and editing. S.A.: Writing—review and editing,supervision, project administration, and funding acquisition. M.A.E.: supervision and writing—review and editing, methodology, formal analysis, resources, data curation. All authors have read and agreed to the published version of the manuscript.

**Funding:** This research was funded by the Deanship of Scientific Research at Princess Nourah Bint Abdulrahman University through the Fast-track Research Funding Program.

**Acknowledgments:** This research was funded by the Deanship of Scientific Research at Princess Nourah bint Abdulrahman University through the Fast-track Research Funding Program.

**Conflicts of Interest:** The authors declare no conflict of interest.

## References

1. Sathya, P.; Kayalvizhi, R. Modified bacterial foraging algorithm based multilevel thresholding for image segmentation. *Eng. Appl. Artif. Intell.* **2011**, *24*, 595–615. [CrossRef]
2. Patra, D.K.; Si, T.; Mondal, S.; Mukherjee, P. Breast DCE-MRI segmentation for lesion detection by multi-level thresholding using student psychological based optimization. *Biomed. Signal Process. Control* **2021**, *69*, 102925. [CrossRef]
3. Bhandari, A.K.; Singh, V.K.; Kumar, A.; Singh, G.K. Cuckoo search algorithm and wind driven optimization based study of satellite image segmentation for multilevel thresholding using Kapur's entropy. *Expert Syst. Appl.* **2014**, *41*, 3538–3560. [CrossRef]
4. Zhang, Z.; Yin, J. Bee Foraging Algorithm Based Multi-Level Thresholding For Image Segmentation. *IEEE Access* **2020**, *8*, 16269–16280. [CrossRef]
5. Tan, K.S.; Isa, N.A.M. Color image segmentation using histogram thresholding–Fuzzy C-means hybrid approach. *Pattern Recognit.* **2011**, *44*, 1–15.
6. Zhou, C.; Tian, L.; Zhao, H.; Zhao, K. A method of two-dimensional Otsu image threshold segmentation based on improved firefly algorithm. In Proceedings of the 2015 IEEE International Conference on Cyber Technology in Automation, Control, and Intelligent Systems (CYBER), Shenyang, China, 8–12 June 2015; pp. 1420–1424.
7. Xing, Z. An improved emperor penguin optimization based multilevel thresholding for color image segmentation. *Knowl.-Based Syst.* **2020**, *194*, 105570. [CrossRef]
8. Arora, S.; Acharya, J.; Verma, A.; Panigrahi, P.K. Multilevel thresholding for image segmentation through a fast statistical recursive algorithm. *Pattern Recognit. Lett.* **2008**, *29*, 119–125. [CrossRef]
9. Otsu, N. A threshold selection method from gray-level histograms. *IEEE Trans. Syst. Man Cybern.* **1979**, *9*, 62–66. [CrossRef]
10. Kapur, J.N.; Sahoo, P.K.; Wong, A.K. A new method for gray-level picture thresholding using the entropy of the histogram. *Comput. Vis. Graph. Image Process.* **1985**, *29*, 273–285. [CrossRef]
11. Maitra, M.; Chatterjee, A. A hybrid cooperative–comprehensive learning based PSO algorithm for image segmentation using multilevel thresholding. *Expert Syst. Appl.* **2008**, *34*, 1341–1350. [CrossRef]
12. Abualigah, L.; Diabat, A.; Mirjalili, S.; Abd Elaziz, M.; Gandomi, A.H. The arithmetic optimization algorithm. *Comput. Methods Appl. Mech. Eng.* **2020**, *376*, 113609. [CrossRef]
13. Garcia-Lamont, F.; Cervantes, J.; López, A.; Rodriguez, L. Segmentation of images by color features: A survey. *Neurocomputing* **2018**, *292*, 1–27. [CrossRef]
14. Zhao, W.; Wang, L.; Zhang, Z. Artificial ecosystem-based optimization: A novel nature-inspired meta-heuristic algorithm. *Neural Comput. Appl.* **2020**, *32*, 9383–9425. [CrossRef]
15. Storn, R.; Price, K. Differential evolution—A simple and efficient heuristic for global optimization over continuous spaces. *J. Glob. Optim.* **1997**, *11*, 341–359. [CrossRef]
16. Naji Alwerfali, H.S.; Al-qaness, M.A.; Abd Elaziz, M.; Ewees, A.A.; Oliva, D.; Lu, S. Multi-Level Image Thresholding Based on Modified Spherical Search Optimizer and Fuzzy Entropy. *Entropy* **2020**, *22*, 328. [CrossRef] [PubMed]
17. Horng, M.H. Multilevel thresholding selection based on the artificial bee colony algorithm for image segmentation. *Expert Syst. Appl.* **2011**, *38*, 13785–13791. [CrossRef]
18. Yousri, D.; Abd Elaziz, M.; Mirjalili, S. Fractional-order calculus-based flower pollination algorithm with local search for global optimization and image segmentation. *Knowl.-Based Syst.* **2020**, *197*, 105889. [CrossRef]

19. Forouzanfar, M.; Forghani, N.; Teshnehlab, M. Parameter optimization of improved fuzzy c-means clustering algorithm for brain MR image segmentation. *Eng. Appl. Artif. Intell.* **2010**, *23*, 160–168. [CrossRef]
20. Omran, M.G.; Salman, A.; Engelbrecht, A.P. Dynamic clustering using particle swarm optimization with application in image segmentation. *Pattern Anal. Appl.* **2006**, *8*, 332. [CrossRef]
21. Elaziz, M.A.; Lu, S. Many-objectives multilevel thresholding image segmentation using knee evolutionary algorithm. *Expert Syst. Appl.* **2019**, *125*, 305–316. [CrossRef]
22. Smith, A. Image segmentation scale parameter optimization and land cover classification using the Random Forest algorithm. *J. Spat. Sci.* **2010**, *55*, 69–79. [CrossRef]
23. Shahrezaee, M. Image segmentation based on world cup optimization algorithm. *Majlesi J. Electr. Eng.* **2017**, *11*. Available online: http://mjee.iaumajlesi.ac.ir/index/index.php/ee/article/view/2213 (accessed on 14 September 2021).
24. Elaziz, M.A.; Oliva, D.; Ewees, A.A.; Xiong, S. Multi-level thresholding-based grey scale image segmentation using multi-objective multi-verse optimizer. *Expert Syst. Appl.* **2019**, *125*, 112–129. [CrossRef]
25. Chakraborty, R.; Verma, G.; Namasudra, S. IFODPSO-based multi-level image segmentation scheme aided with Masi entropy. *J. Ambient. Intell. Humaniz. Comput.* **2021**, *12*, 7793–7811. [CrossRef]
26. Versaci, M.; Morabito, F.C. Image edge detection: A new approach based on fuzzy entropy and fuzzy divergence. *Int. J. Fuzzy Syst.* **2021**, 1–19. [CrossRef]
27. Bhandari, A.K. A novel beta differential evolution algorithm-based fast multilevel thresholding for color image segmentation. *Neural Comput. Appl.* **2020**, *32*, 4583–4613. [CrossRef]
28. Xing, Z.; Jia, H. Modified thermal exchange optimization based multilevel thresholding for color image segmentation. *Multimed. Tools Appl.* **2020**, *79*, 1137–1168. [CrossRef]
29. Sepas-Moghaddam, A.; Yazdani, D.; Shahabi, J. A novel hybrid image segmentation method. *Prog. Artif. Intell.* **2014**, *3*, 39–49. [CrossRef]
30. Mahajan, S.; Mittal, N.; Pandit, A.K. Image segmentation using multilevel thresholding based on type II fuzzy entropy and marine predators algorithm. *Multimed. Tools Appl.* **2021**, *80*, 19335–19359. [CrossRef]